

Review

# A Review on Microfluidics-Based Impedance Biosensors

Yu-Shih Chen <sup>1</sup> , Chun-Hao Huang <sup>1</sup>, Ping-Ching Pai <sup>2</sup>, Jungmok Seo <sup>1,3,\*</sup>  and Kin Fong Lei <sup>1,2,3,\*</sup> <sup>1</sup> Department of Biomedical Engineering, Chang Gung University, Taoyuan 33302, Taiwan<sup>2</sup> Department of Radiation Oncology, Linkou Chang Gung Memorial Hospital, Taoyuan 33305, Taiwan<sup>3</sup> Department of Electrical & Electronic Engineering, Yonsei University, Seoul 120-749, Republic of Korea

\* Correspondence: jungmok.seo@yonsei.ac.kr (J.S.); kflei@mail.cgu.edu.tw (K.F.L.)

**Abstract:** Electrical impedance biosensors are powerful and continuously being developed for various biological sensing applications. In this line, the sensitivity of impedance biosensors embedded with microfluidic technologies, such as sheath flow focusing, dielectrophoretic focusing, and interdigitated electrode arrays, can still be greatly improved. In particular, reagent consumption reduction and analysis time-shortening features can highly increase the analytical capabilities of such biosensors. Moreover, the reliability and efficiency of analyses are benefited by microfluidics-enabled automation. Through the use of mature microfluidic technology, complicated biological processes can be shrunk and integrated into a single microfluidic system (e.g., lab-on-a-chip or micro-total analysis systems). By incorporating electrical impedance biosensors, hand-held and bench-top microfluidic systems can be easily developed and operated by personnel without professional training. Furthermore, the impedance spectrum provides broad information regarding cell size, membrane capacitance, cytoplasmic conductivity, and cytoplasmic permittivity without the need for fluorescent labeling, magnetic modifications, or other cellular treatments. In this review article, a comprehensive summary of microfluidics-based impedance biosensors is presented. The structure of this article is based on the different substrate material categorizations. Moreover, the development trend of microfluidics-based impedance biosensors is discussed, along with difficulties and challenges that may be encountered in the future.

**Keywords:** microfluidic; impedance biosensor; electrical impedance flow cytometer; electrochemical impedance spectroscopy



**Citation:** Chen, Y.-S.; Huang, C.-H.; Pai, P.-C.; Seo, J.; Lei, K.F. A Review on Microfluidics-Based Impedance Biosensors. *Biosensors* **2023**, *13*, 83. <https://doi.org/10.3390/bios13010083>

Received: 21 November 2022

Revised: 20 December 2022

Accepted: 28 December 2022

Published: 3 January 2023



**Copyright:** © 2023 by the authors. Licensee MDPI, Basel, Switzerland. This article is an open access article distributed under the terms and conditions of the Creative Commons Attribution (CC BY) license (<https://creativecommons.org/licenses/by/4.0/>).

## 1. Introduction

Biosensors are mainly used to measure or perceive signals from biological responses. Electrical biosensors can be generally classified into potential, current, and impedance sensors [1]. H. E. Ayliffe pioneered the measurement of single-cell impedance in a microchannel in 1999 [2]. Biological substances can be detected using a pair of microelectrodes with a gap of several  $\mu\text{m}$ , in a microchannel 10  $\mu\text{m}$  in width. This narrow microchannel allowed for a more accurate impedance measurement of human polymorphonuclear leukocytes and teleost fish red blood cells. Subsequently, the electrical and equivalent circuit models of single cells were established [3,4].

As early as 1984, Giaever et al. designed a device on a Petri dish that could monitor impedance in order to investigate the density and cell migration of fibroblasts [5]. The impedance signal was obtained by gold electrodes 130  $\mu\text{m}$  in width, which were deposited by a metal evaporator using a mask. Fibroblasts were attached to the gold electrodes, and their cellular response could be represented by the impedance measured across the electrodes [6]. The measured impedance values could differentiate normal fibroblasts from transformed cells. When fibronectin and gelatin were coated on the gold electrodes, the fibroblasts showed a better response. Based on the results of electrical signal monitoring, cell movement was observed. Later, Giaever published an article proposing that the phenomenon of cell movement is called micromotion [7], following which the authors

put forward a mathematical model establishing the theory of cell movement analysis. Experimentally, small fluctuations in impedance electrical signals were measured as direct evidence of cell movement. Unlike cells observed by light microscopy, impedance biosensors are designed to continuously track the vertical movement of detected cells [8]. The range of cell motion can be as small as 1 nm. The impedance value and fluctuation of each type of cell differs and, so, may be used as a cell fingerprint. Regarding electrical impedance spectroscopy, Grossi et al. carried out a series of literature reviews [9]. The impedance spectrum is usually matched with an equivalent circuit model, and the impedance spectrum obtained by each test object can be expressed as the electrical fingerprint of the test object. Sun et al. used electrochemical impedance spectroscopy to explain the dielectric properties of individual polyelectrolyte microcapsules with different shell thicknesses [10]. The authors built a complete equivalent circuit model of a single solid spherical particle in suspension, and the resistance of the shell and the capacitance of the inner core were used to determine the permittivity and conductivity of individual capsule shells. The study indicated that the conductivity of the six- and nine-layer microcapsule shells could be estimated as  $28 \pm 6$  and  $3.3 \pm 1.7 \text{ mS m}^{-1}$ , respectively.

On the other hand, the first microchannel-based flow cytometer was designed by Kamentsky et al. in 1965 [11], with a cell throughput of 500 cells per second. Initially, optical detection was used, using wavelengths of 253 nm and 410 nm. Later on, S. Gawad developed an impedance spectroscopy flow cytometer using Pt as an electrode, which could reduce the electrode impedance and allow the measurement frequency to be as low as 10 kHz [12]. By using a three-electrode design, the impedance value when the cells pass through can be easily measured. The peak impedance value is related to the cell size, and the electrode spacing and the time difference between two impedance signals could also be used to determine the velocity of the measured particle. Gawad et al. established a model to discriminate cell size, membrane capacitance, and cytoplasmic conductivity using a miniature cytometer [13]. Moreover, Cheung et al. obtained amplitude, opacity, and phase information using a microfluidic impedance cytometer, which can be used to distinguish different cells [14], where the measured amplitude can determine the cell size. Opacity was used to distinguish polystyrene beads from red blood cells (RBCs), while phase information was used to distinguish between RBCs and ghosts. RBCs and RBCs fixed in glutaraldehyde could also be distinguished by opacity. The definition of opacity was published in an article by R. A. Hoffman [15]; in particular, it is the ratio of the high-frequency impedance to low-frequency impedance of a particle. Some scholars have studied the development of fluidic impedance cytometers for micro-single cells [16].

Impedance biosensors integrated with microfluidic technology can be categorized into two major technologies: electrical impedance flow cytometry and electrochemical impedance spectroscopy. In the design of a microchannel, an electrical impedance flow cytometer can measure dynamic objects using impedance technology. On the other hand, electrochemical impedance spectroscopy is usually combined with microcavity structures. Static objects can be measured using impedance measurement techniques. In this review article, microfluidics-based impedance biosensors are comprehensively summarized and classified according to the different substrate materials. The development trend, difficulties, and challenges associated with microfluidics-based impedance biosensors, which are expected to be encountered in the future, are also discussed.

## 2. Silicon-Based Impedance Biosensors

Silicon-based impedance biosensors are only possible with the fabrication of the electrodes by micromachining. Therefore, the development of silicon impedance biosensors began earlier; however, a number of articles have also been published recently, due to relevant special processes.

An impedance biosensor with a nanometer-wide interdigitated electrode array was developed [17], with electrode widths and spacings of 250–500 nm microfabricated using deep UV lithography. The same article also verified the binding of biomolecular structures

to nanoscale electrode surfaces. The impedance signal results indicate that the immobilization of glucose oxidase on the electrode can be monitored. A silicon-based microfabricated biochip was designed to measure the electrical impedance spectrum [18], which could measure the conductance change in a 30 nl volume of bacterial suspension and showed the viability of the bacteria. The same research demonstrated electrical impedance values for the live micro-organism *Listeria innocuous*. By-products after bacterial metabolism have also been shown to change the electrical impedance value; for example, Radke et al. developed an impedance biosensor for bacterial detection using immobilized antibodies. The interdigitated electrode arrays were designed on silicon-based biosensors [19]. *Escherichia coli*-specific antibodies were immobilized on the electrodes, and impedance changes due to bacteria immobilized on the interdigitated gold electrodes were observed. Impedance signals at low frequencies showed that bacteria bound to the sensor electrode surface within 5 min. The rate of binding was the most pronounced in the first 20 min but slowed down significantly after 35 min. At high frequencies, impedance does not change over time. Test concentrations can be as low as 10 CFU/mL of bacterial suspension. The same research team used an impedance biosensor with immobilized antibodies and interdigitated electrode arrays to detect pathogenic *Escherichia coli* O157:H7 and *Salmonella* infants [20]. It mainly detects bacteria in food or water. P-type (100) silicon wafers were used in that article. Coplanar impedance sensors were designed on glass and fabricated by photolithography [21]. They verified that the spacing of the set of coplanar electrodes is a more important parameter than the electrode area. As the spacing of the electrode design increases, the impedance value increases accordingly. An impedance sensor was used to monitor drug-affected spheroids in a microcavity [22]. Silicon wafers were microfabricated into microcavities through wet anisotropic etching. The impedance sensor was designed with 15 microcavities, and 4 electrodes in each cavity were used to sense the impedance of the spheroids. OLN93 cell spheroids were most loosely organized and peaked at around 180 kHz, while Bro cell spheroids had a more compact structure and showed a peak at 100 kHz. They also observed the impedance of the spheroids 8 h after drug administration. Impedance increased with forskolin, camptothecin, and staurosporine and decreased with doxorubicin and tamoxifen. Single-cell impedance and optical sensing were integrated into a single chip for real-time viability assessment [23]. Single-cell capture microwell chips were obtained by etching silicon wafers with KOH. The induction chip is composed of two cavities (upper and lower). The adhesion changes of RAW264.7 macrophages can be assessed through the impedance value of the sensing chip. In an interdigitated electrode array, the gap between the electrodes is an important factor to improve the sensitivity of the biosensor [24]. Three-dimensional interdigitated electrode arrays were fabricated to sense the impedance signals of proteins. C-reactive protein-specific antibodies were immobilized on the electrode surface. The results showed that electrochemical impedance spectroscopy can be used to monitor the concentration of C-reactive protein in human serum. An impedance biosensor that can sense the concentration of picesterol was developed [25]. The electrodes on the silicon wafer were designed with interdigitated electrodes, where the distance between two electrodes was 15  $\mu\text{m}$ . Cortisol-specific monoclonal antibodies were immobilized on the surface of the microelectrodes. Cortisol binding to antibodies can be signaled by changing the impedance values. The experimental results showed that the impedance biosensor can accurately detect cortisol in the range of 1 pM to 10 nM in saliva. An electrical impedance biosensor was constructed through a CMOS-process, using high-density sensing electrodes for the detection of breast tumor cells (MCF-7) [26]. A total of  $96 \times 96$  gold microelectrodes were designed with a sensing area of  $3.5 \text{ mm} \times 3.5 \text{ mm}$ . The impedance signal is read out by an integrated circuit fabricated with 0.18  $\mu\text{m}$  CMOS technology. The results showed that the increase in impedance was associated with cell binding to the electrode surface. Ma et al. designed an impedance biosensor that can detect suspended DNA, as shown in Figure 1a [27], where the sensing electrodes are fabricated using 0.35  $\mu\text{m}$  CMOS technology. They proposed that the impedance of a solution is highly dependent on the concentration. Moreover, the impedance value of the sample

solution is also highly correlated with the length of the DNA fragment. In other words, the biological samples obtained after PCR can be tested using the biosensors designed in that article. Lisandro Cunci developed electrochemical impedance biosensors that can detect telomerase in cancer cells [28]. The flexible heater and temperature sensor were designed together in the biosensor. Single-stranded DNA probes were immobilized on the surface of the interdigitated gold electrode array. Jurkat cells were tested for telomerase and showed a 14-fold increase in electrical resistance. The sensitivity of electrochemical impedance spectroscopy biosensors was enhanced using electric field focusing of magnetic beads in microwells [29], where the antibody is immobilized on the surface of the magnetic beads. Microwells are fabricated on silicon wafers using high aspect ratio SU-8 microstructures. In the same article, prostate-specific antigen in a PBS buffer and human plasma were used to validate the argument that focused magnetic beads can improve the sensitivity. The experimental results showed that prostate-specific antigens at low concentrations (i.e., tens or hundreds of fg/mL) could be detected. Pursey et al. integrated surface plasmon resonance and electrochemical impedance spectroscopy into a microfluidic chip, targeting bladder cancer-associated DNA sequences, as shown in Figure 1b [30]. Gold electrodes are microfabricated on the silicon layer, and 20 sensors on the same wafer simultaneously detect three different DNA markers for bladder cancer. Signals were measured within a short period of 20 min. Impedance biosensors that can monitor bacteria have also been developed. In one study, 216 three-dimensional interdigitated electrodes of 3  $\mu\text{m}$  width and with 3  $\mu\text{m}$  gap were microfabricated on a silicon wafer [31]. To improve the sensitivity, the three-dimensional electrodes were separated by an insulating layer. In addition to sensing the impedance signals of bacteria, the three-dimensional electrode can also concentrate bacteria. An impedance sensor fabricated in microgrooves was developed, where silicon substrates were microfabricated to create the microgrooves, as shown in Figure 1c [32]. Two gold electrodes were microfabricated in the microgrooves, which can be used to sense the impedance value of three-dimensional cancer cells, and changes in impedance can reflect the proliferation and apoptosis of three-dimensional cancer cells. Impedance sensors can also identify cancer cells that are affected by drugs. A biosensor combining impedance and photoelectrochemical analysis of cancer cells was designed, as shown in Figure 1d [33], where monocrystalline silicon was used as a substrate for the biosensor. The serrated interdigitated electrodes not only can focus cells but also sense impedance signals. They identified four different types of cancer cells: esophageal cancer (CE81T cell), esophageal cancer (OE21 cell), lung adenocarcinoma (A549 cell), and bladder cancer (TSGH-8301 cell).

The development of silicon chips for microfluidic impedance sensors depends on the development of the microelectromechanical system. Many silicon-based microfabrication processes and metal microelectrode processes are derived from microelectromechanical system microfabrication. Therefore, this is discussed in the first part of this article. Due to the special process requirements, several articles have focused on silicon-based microfluidic impedance sensors. In recent years, the COVID-19 virus has spread throughout the world, and this multi-mutated virus needs to be sensed through the use of biosensors. The MEMS process developed by Taiwan's Taiwan Semiconductor Manufacturing Company may provide the direction for such a technology to be commercialized.

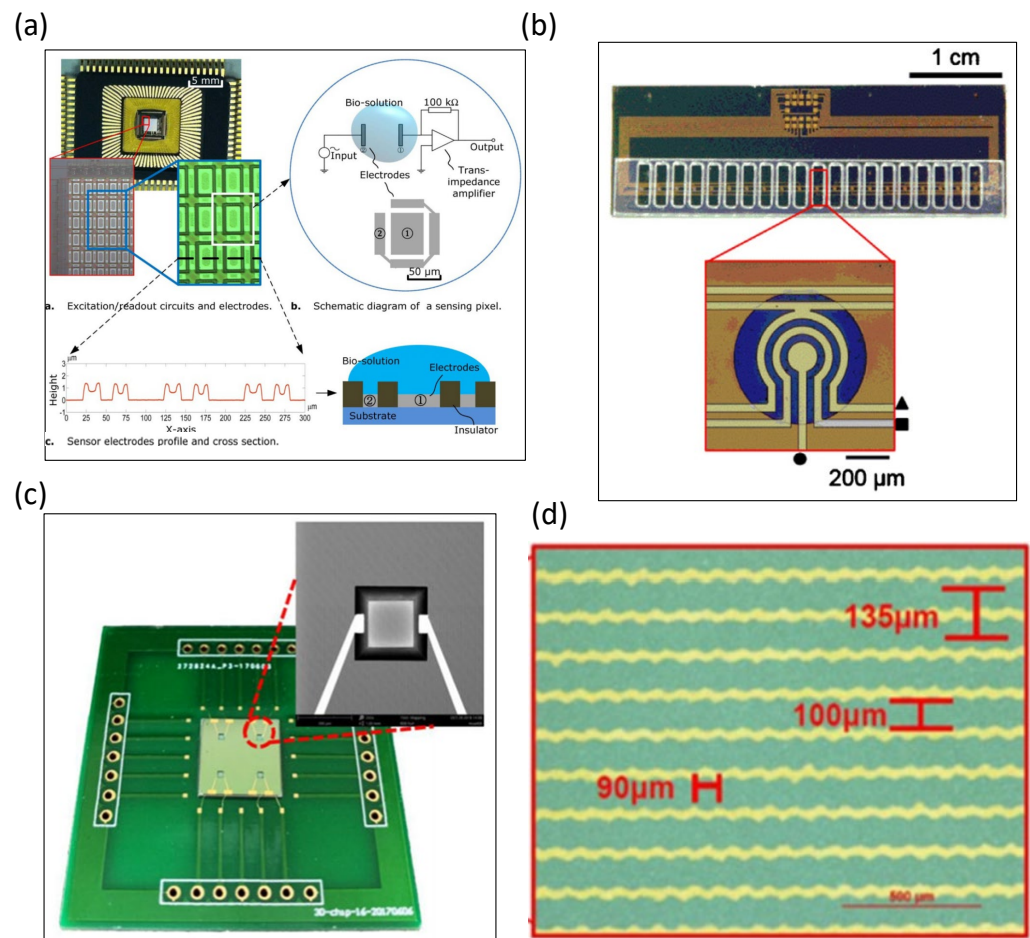


**Figure 1.** The silicon-based impedance biosensors. (a) A low-cost 0.35 mm CMOS technology by TSMC (Taiwan) was used to fabricate the micro-array chip that sensed DNA characterization. Reproduced with permission from [27]. Copyright Scientific Reports 2013. (b) Integrated surface plasmon resonance and electrochemical impedance spectroscopy in a microfluidic chip [30]. Reproduced with permission from [30]. Copyright Sensors and Actuators B: Chemical 2017. (c) Silicon substrates were microfabricated to create microgrooves. Reproduced with permission from [32]. Copyright Microsystems and Nanoengineering 2020. (d) A biosensor combining impedance and photoelectrochemical was designed. Reproduced with permission from [33]. Copyright Biosensors 2022.

### 3. Printed Circuit Board (PCB)-Based Impedance Biosensors

Printed circuit boards (PCBs) are flat plates that were originally used to make circuits, which are very commercialized. Their electrode width and electrode spacing are not very small; therefore, the sensitivity limit of the sensor is not low either.

Electrochemical impedance spectroscopy biosensors consist of PCBs with gold-coated electrodes, which are mainly used to detect plant pathogens [34], where the antibody is first bound to the surface of the electrochemical sensor. For papaya ring spot virus, the biosensor was shown to be capable of detecting papaya ring spot virus coat protein with high sensitivity. A chip using a microfluidic impedance sensing system to detect the transgenic protein Cry1Ab was designed, as shown in Figure 2a [35]. Gold electrodes were printed on commercial printed circuit boards, with the spacing between two printed electrodes being 250  $\mu\text{m}$ . The impedance signal at the optimal test frequency (358.3 Hz) presented a good linear relationship with the concentration of the transgenic protein Cry1Ab in the range of 0–0.2 nM. Clinically, the degree of red blood cell agglutination is divided into five grades by visual inspection, which is routinely conducted in hospitals [36]. An electrical impedance blood-sensing chip was designed by Chang et al. to distinguish the degree of blood agglutination. The interdigitated electrode array was designed on a PCB.

ZnO nanowires were synthesized on the surface of the electrode array in order to improve the sensitivity of impedance measurement. An electrical impedance sensor was used to detect the degree of fibrosis in liver tissue, as shown in Figure 2b [37], where liver tissue was detected by a pair of gold electrodes on the PCB. The experimental results indicate that the maximum resistance difference between healthy and fibrotic tissue was about 2 k $\Omega$  at day 8.

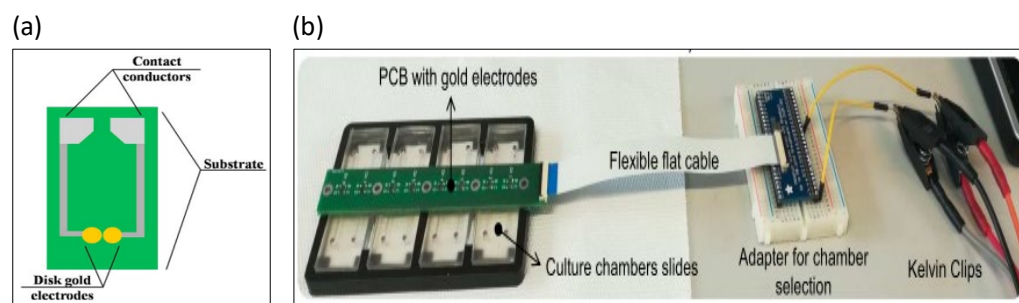


**Figure 2.** The PCB-based impedance biosensors. (a) Gold electrodes were printed on commercial printed circuit boards. Reproduced with permission from [35]. Copyright Scientific Reports 2013. (b) An electrical impedance sensor was used to detect the degree of fibrosis in liver tissue. Reproduced with permission from [37]. Copyright Biosensors 2022.

The development of PCB chips is limited by the electrode line width in traditional PCB processes. Microelectrodes that are not tiny enough will lead to an inability to improve the sensitivity. Therefore, PCB chips are more suitable for the production or commercial design where the induction is fast and the sensitivity requirements are not high.

#### 4. Polymer-Based Impedance Biosensors

In addition to glass, the most commonly used substrates in the field of microfluidics are polymer chips. Different from the stretchable chips mentioned in later chapters, the polymer chips mentioned in this chapter are formed of hard and inflexible materials.

A study considering electrochemical impedance spectroscopy on polymer substrates was developed [38], in which the authors designed a nanoscale interdigitated electric shock array, in which the electrode width was only 200 nm and the electrode spacing was 500 nm. Gold nanometer interdigitated electrode arrays were patterned on cyclic olefin copolymer substrates. Experiments have demonstrated selective iDEP capture and impedance detection on polystyrene microspheres and *Bacillus subtilis* spores [39]. The authors used oxides to passivate the sensing electrode of the sensor in order to avoid the metal and electrolyte having adverse effects on the electrode surface. Cyclic olefin copolymer was used as the substrate of the sensor. Studies have used all-polymer electrochemical microfluidic biosensors for electrochemical impedance spectroscopy, as shown in Figure 3a [40], where polymer materials from Topas Corporation were used as substrates and conductive polymer bilayers were used as electrode materials. Electrochemical impedance spectroscopy was able to detect ampicillin in a concentration range from 100 pM to 1  $\mu$ M and kanamycin A from 10 nM to 1 mM. Figure 3b shows how Pires et al. combined an impedance sensor and a current sensor to detect biofilms in water [41]. Two microfluidic chambers were designed on a cyclic olefin copolymer substrate with four impedance sensors and three current sensors in each cavity. A conductive polymer (PEDOT:TsO) was fabricated as an interdigitated electrode array for impedance biosensors [42], where the cyclic olefin copolymer produced by TOPAS was used as the base material for the conductive polymer electrodes. A microfluidic impedance sensor was used to detect the food additive clenbuterol hydrochloride [43], where the electrodes were patterned on poly (ethylene terephthalate) films. Polyaniline@graphene oxide nanocomposites were used to functionalize the sensing electrodes, and the microfluidic impedance sensors could detect down to 0.12 ppb. Sharif et al. integrated a microfluidic system and a magnetic separation procedure

to develop a novel impedance sensor for the detection of various foodborne pathogens [44]. Their results showed that the impedance sensor was effective for the detection of various foodborne pathogens, including *Escherichia coli* (*E. coli* O157:H7), *Vibrio parahaemolyticus* (*V. parahaemolyticus*), *Staphylococcus aureus* (*S. aureus*), and *Listeria monocytogenes* (*L. monocytogenes*). Polymethyl methacrylate (PMMA) was used as the substrate. D-dimer is a biomarker in the blood that can be used to diagnose deep vein thrombosis and pulmonary embolism [45]. Lakey et al. designed a polymer microfluidic impedance sensor for the detection of D-dimer, where interdigitated electrode arrays were patterned on polyethylene naphthalate (PEN) substrates. Ma et al. developed an electrochemical impedance spectroscopy approach for the detection of endotoxins [46]. The electrodes were screen-printed on a polyethylene terephthalate (PET) substrate, which contained carbon for the working and auxiliary electrodes and Ag/AgCl for the reference electrode. The sensitivity of the impedance biosensors could be as low as  $500 \text{ pg mL}^{-1}$ , and the total measurement time was only half an hour. Niaraki et al. used graphene microelectrodes to monitor neuronal growth and detachment after death, as shown in Figure 3c [47]. Kapton Polyimide (PI) was used as a substrate for patterned graphene electrodes. The microelectrodes fabricated by this research team feature a wrinkled surface morphology, which allows for a fast response time to be achieved. Chmayssem et al. integrated a cell culture chamber with electrochemical impedance spectroscopy, as shown in Figure 3d [48]. The researchers used a screen-printing technique to fabricate the microelectrodes on polyethylene terephthalate (PET) sheets. The electrode material was selected, and Ag/AgCl was used as the low interface impedance electrode on the PET sheet. On the top layer of electrodes was carbon-biocompatible ink rich in IrOx particles. Hantschke et al. integrated electrophoretic and electrical impedance sensors for point-of-care (POC) diagnostics [49], where the electrodes and microchannels were fabricated on polymethylmethacrylate (PMMA) substrates.

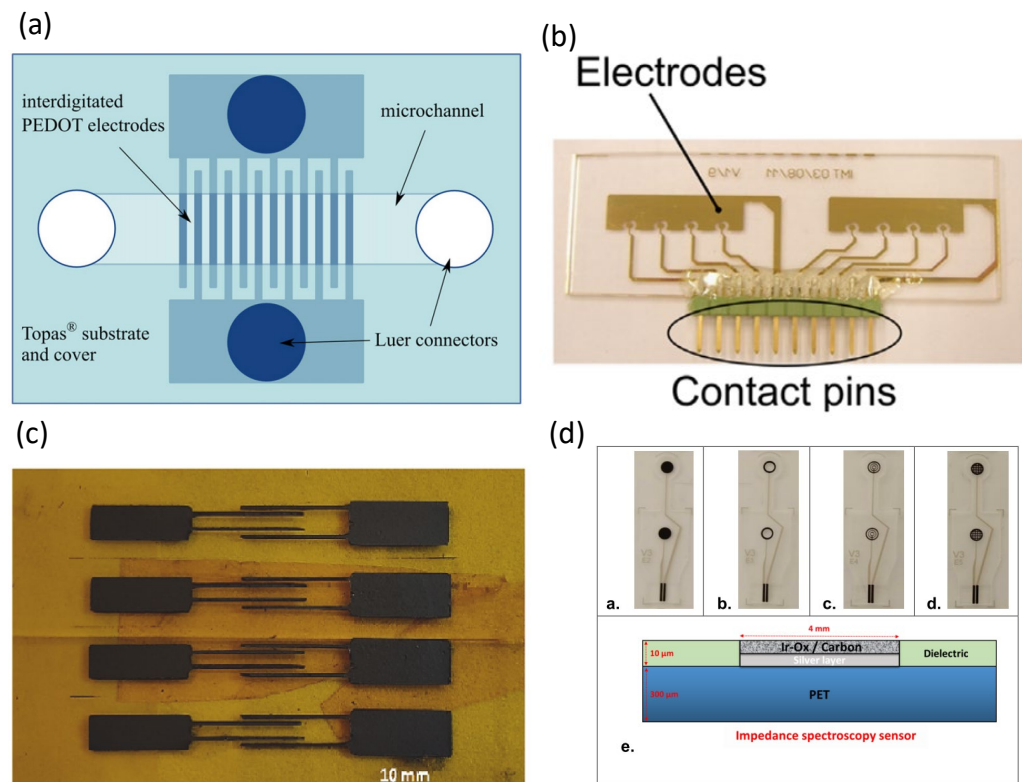


**Figure 3.** The polymer-based impedance biosensors. (a) All-polymer electrochemical microfluidic

biosensors are used. Reproduced with permission from [40]. Copyright Biosensors and Bioelectronics 2013. (b) Two microfluidic chambers were designed on a cyclic olefin copolymer substrate. Reproduced with permission from [41]. Copyright Biosensors and Bioelectronics 2013. (c) Kapton Polyimide (PI) was used as a substrate. Reproduced with permission from [47]. Copyright Biosensors and Bioelectronics 2022. (d) Microelectrodes were microfabricated on polyethylene terephthalate (PET) sheets. Reproduced with permission from [48]. Copyright Biosensors 2022.

The key to the use of polymer chips in microfluidic impedance biosensors is the combination of microelectrodes and polymer substrates. The sensitivity of the biosensors were determined by the size of the microelectrodes. Polymer chips are used similarly to glass chips, with both being hard and inelastic materials. On the other hand, polymer materials are suitable for mass production. Therefore, polymer chips can be one of the options for commercialization.

## 5. Glass-Based Impedance Biosensors

Microfluidic chips with glass as the substrate are very common. There have been some articles on materials that can replace glass, such as ITO glass, Pyrex glass, and SiO<sub>2</sub> glass. Therefore, the classification in this chapter is based on what the biosensors on glass can monitor. In this line, the subsections are classified regarding the detection of bacteria, blood, cells, DNA, proteins, toxins, and viruses.

### 5.1. Detection of Bacteria

Ruan et al. used electrochemical impedance spectroscopy to detect *E. coli* O157:H7 [50]. An anti-*E. coli* O157:H7 antibody was immobilized on the surface of an indium tin oxide (ITO) electrode. The binding of the antibody to the antigen changed the impedance signal. The limit of the sensor to detect bacteria was as low as  $6 \times 10^3$  cells/mL. Yang et al. used an impedance sensor to detect *Salmonella typhimurium* and observed impedance changes during bacterial growth [51]. The material of the interdigitated electrode array was ITO. Four frequencies (10 Hz, 100 Hz, 1 kHz, and 10 kHz) were used to record impedance growth curves in the experiment. The impedance changes only when the bacterial count reaches  $10^5$ – $10^6$  CFU/mL. Experimental data indicated that the greatest impedance change was observed at 10 Hz.  $[\text{Fe}(\text{CN})_6]^{3-/4-}$  was used as a redox probe [52], which increases the electron transfer resistance on the antibody-immobilized microelectrode surface. Impedance immunosensors for the detection of *Listeria* were developed [53], for which TiO<sub>2</sub> nanowires were immobilized on gold electrodes, and monoclonal antibodies were immobilized on the nanowires. *Listeria* was then specifically captured using the antibodies. The impedance immunosensors sense impedance changes induced by the nanowire–antibody–bacteria system. Tan et al. designed a microfluidic impedance immunosensor for the detection of *Escherichia coli* and *Staphylococcus aureus* [54]; in particular, specific antibodies were immobilized on alumina nanoporous membranes, and bacteria were captured on the nanoporous membranes by antibodies. In a 2 h rapid assay, the sensitivity was as high as  $10^2$  CFU/mL. J. Lum designed an impedance biosensor, mainly for avian influenza virus subtype H5N1, as shown in Figure 4a [55]. Immunomagnetic nanoparticles and interdigitated microelectrodes were designed on a microfluidic chip. The polyclonal antibody was immobilized on the surface of the microelectrode, which binds to the avian influenza virus H5N1 to generate an impedance signal. Chicken red blood cells were used as biomarkers attached to the interdigital microelectrodes. The results showed that the impedance signal was increased by more than 100%. An impedance biosensor with focusing and sensing electrodes was designed to detect *E. coli* O157:H7 [56]. The sensitivity lower limit of detection for impedance sensor measurements was  $3 \times 10^2$  CFU/mL. By focusing on p-DEP, the measurement sensitivity can be increased by 2.9 to 4.5 times. Couniot et al. integrated a CMOS process to design an impedance sensor for bacterial detection in urine, as shown in Figure 4b [57], where the detection of impedance spectroscopy was mainly directed at *Staphylococcus epidermidis*. Pyrex wafers were used as substrates for the impedance sensors. Liu et al. developed impedance-based biosensors that can be used to simultane-

ously detect Salmonella Serotypes B, D, and E by relying on three sensing IDE arrays, as shown in Figure 4c [58]. The sensor was designed with focusing electrodes to generate dielectrophoretic force, where the focusing force can increase the sensitivity by 4–4.5 times, and the detection limit is as low as 8 cells/mL. Other results indicated that the sensor could also distinguish between dead and live cells. Dastider et al. designed a microfluidic impedance sensor that can sense low concentrations of *E. coli* O157:H7 [59]. Upstream of the microchannel, the authors designed interdigitated focusing electrodes, in which the electrodes were arranged in a 45-degree-inclined manner. Positive DEP forces were used to focus cells in the center of the microchannel. Then, downstream of the microchannel, three sets of interdigital electrode arrays (IDEAs) were designed to sense impedance. An *E. coli* antibody was functionalized on the sensing electrode, which captured *E. coli* and resulted in a change in impedance. Experiments have shown that the microfluidic impedance sensor can detect coliform bacteria at a concentration of 39 CFU/mL. A microfluidic impedance sensor was used to detect Salmonella Serotypes B and D in food, as shown in Figure 4d [60]. There are two sensing areas in the chip, and the sensing electrodes are composed of interdigitated electrodes. The shocks were coated with antibodies against Salmonella. The experimental results demonstrate that the impedance sensor can detect Salmonella as low as 300 cells/mL.

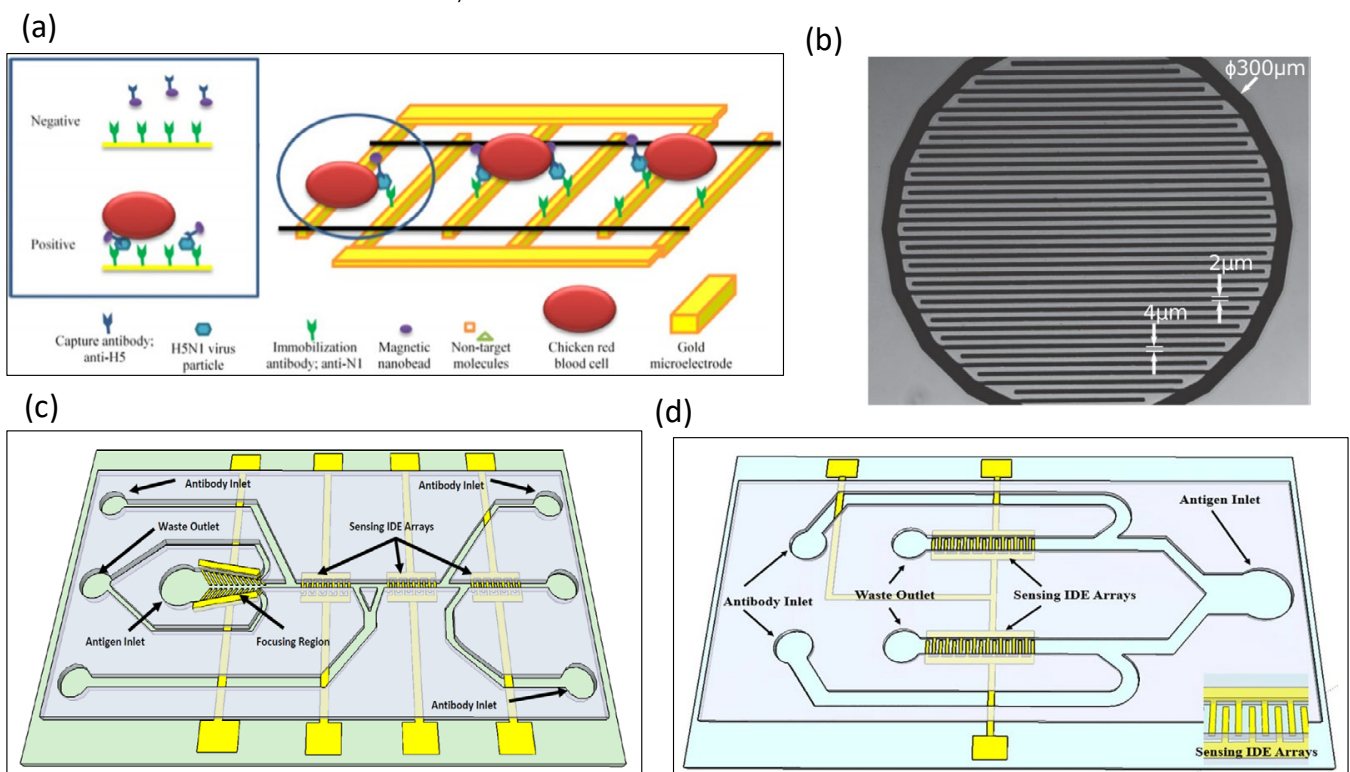


**Figure 4.** Glass-based impedance biosensors for detecting bacteria. (a) A polyclonal antibody was immobilized on the surface of a microelectrode and bound to avian influenza virus H5N1 to generate an impedance signal. Reproduced with permission from [55]. Copyright Biosensors and Bioelectronics 2012. (b) Pyrex wafers were used as substrates for impedance sensors. Reproduced with permission from [57]. Copyright Biosensors and Bioelectronics 2015. (c) An impedance-based biosensors were used to simultaneously detect Salmonella Serotypes B, D, and E. Reproduced with permission from [58]. Copyright Scientific Reports 2018. (d) There were two sensing areas in the chip, and the sensing electrodes were composed of interdigitated electrodes. Reproduced with permission from [60]. Copyright PLoS ONE 2019.

Many of the keys aspects in the design of impedance biosensors used to sense bacteria are related to improving the sensitivity. As the combination of antigen and antibodies

can lead to changes in the impedance signal, many studies on antibodies immobilized on electrodes have been carried out.

### 5.2. Detection of Blood Samples

The manufacturing of electrical impedance measurement systems became possible with microfabrication technology. For example, wet etching was used to obtain microchannels on a coverslip [2], and gold electrodes were plated on both sides of the microchannel. The authors scanned the electric impedance spectroscopy of ionic salt solutions, air, and deionized (DI) water in the frequency range from 100 Hz to 2 MHz. Their experimental results showed the efficacy of electrical impedance spectroscopy for human polymorphonuclear leukocytes and teleost fish red blood cells. Mishra et al. used three microelectrodes on a chip to sense the impedance of human CD4(+) cells in blood, as shown in Figure 5a [61]. The reference electrode, working electrode, and counter electrode were microfabricated on glass wafers. As the protein adsorbed onto the microelectrode surface, the detected impedance value increased even more. The impedance also increased with the number of captured cells. Kuttel et al. used impedance spectroscopy to detect red blood cells infected with *Babesia bovis* [62]. The change in impedance was mainly due to the presence of the parasite in the cell changing the impedance value of the original red blood cells, white blood cells, or platelets. Therefore, infected cells could be easily and quickly distinguished from healthy cells. In areas without good infrastructure or in very remote areas, the use of impedance spectroscopy to detect parasites in whole blood samples can greatly reduce the time of diagnosis for medical personnel. Holmes et al. developed a high-speed microfluidic single-cell impedance cytometer using dual frequency for whole blood analysis [63], which is mainly used for the impedance measurement and identification of T lymphocytes, monocytes, and neutrophils. The experiments showed that, at low frequencies, T lymphocytes and neutrophils can be distinguished. The cells were conjugated with fluorescently labeled antibodies, allowing the system to analyze fluorescence and impedance simultaneously. Han et al. developed a microfluidic chip that integrates red blood cell lysis with a microfluidic impedance cytometer, as shown in Figure 5b [64]. Their laboratory developed a buffer that not only lyses red blood cells but also increases the identification of monocytes and neutrophils. The method for multi-step cell lysis described in this paper is of great help for the microfluidic system, in terms of whole blood analysis. Lei et al. designed an electrical impedance to monitor the blood coagulation process in a microfluidic chip, which can obtain impedance results consistent with clinical reports at different temperatures and blood cell counts, as shown in Figure 5c [65]. This device provides a new analytical method for the sensitive and real-time monitoring of coagulation in whole blood samples. Song et al. developed a microfluidic impedance flow cytometer to identify undifferentiated and differentiated mouse embryonic stem cells [66], where two micropores and three electrodes were designed in the chip. The experimental results indicated that undifferentiated stem cells and polystyrene spheres could be distinguished at any frequency, while undifferentiated and differentiated stem cells require higher frequency and opacity to be distinguished. Du et al. designed an electrical impedance flow cytometer targeting red blood cells infected with *Plasmodium falciparum* [67]. The physiological and electrical properties of erythrocytes were altered 48 h after *P. falciparum* infection. In addition to the cytometer, the authors incorporated new offset parameters to make it easier to distinguish infected erythrocytes from uninfected erythrocytes. Spencer et al. used a microfluidic impedance cytometer for the detection of a representative circulating tumor cell (the MCF7 tumor cell line) [68]. The red blood cells were removed by lysis, and the buffer did not affect the dielectric properties of the MCF7 cells. Through impedance analysis, MCF7 cells were shown to have a larger size and membrane capacitance. The experimental results indicated that 100 MCF7 cells could be detected in 1 mL of whole blood. The average recovery rate was as high as 92%. Liu et al. developed an electrical impedance microflow cytometer that can control oxygen flow for the analysis of sickle blood cells, as shown in Figure 5d [69]. The two-layer microfluidic channel was separated by a 150  $\mu\text{m}$  thick PDMS film. The upper layer is a ser-

pentine gas channel that controls oxygen, while the lower layer is a microchannel through which sickle cells and red blood cells flow. Ti/Au electrodes were designed to measure the impedance of sickle cells in the lower microchannel. Under normoxic conditions, the authors distinguished between normal and sickle cells using impedance signals measured at intermediate frequencies. The same research demonstrated that impedance signals can be obtained without the need for hemolysis. Their experimental results also proved that the impedance signal of the microflow cytometer can be used as an indicator of red blood cell disease and sickle cell disease.

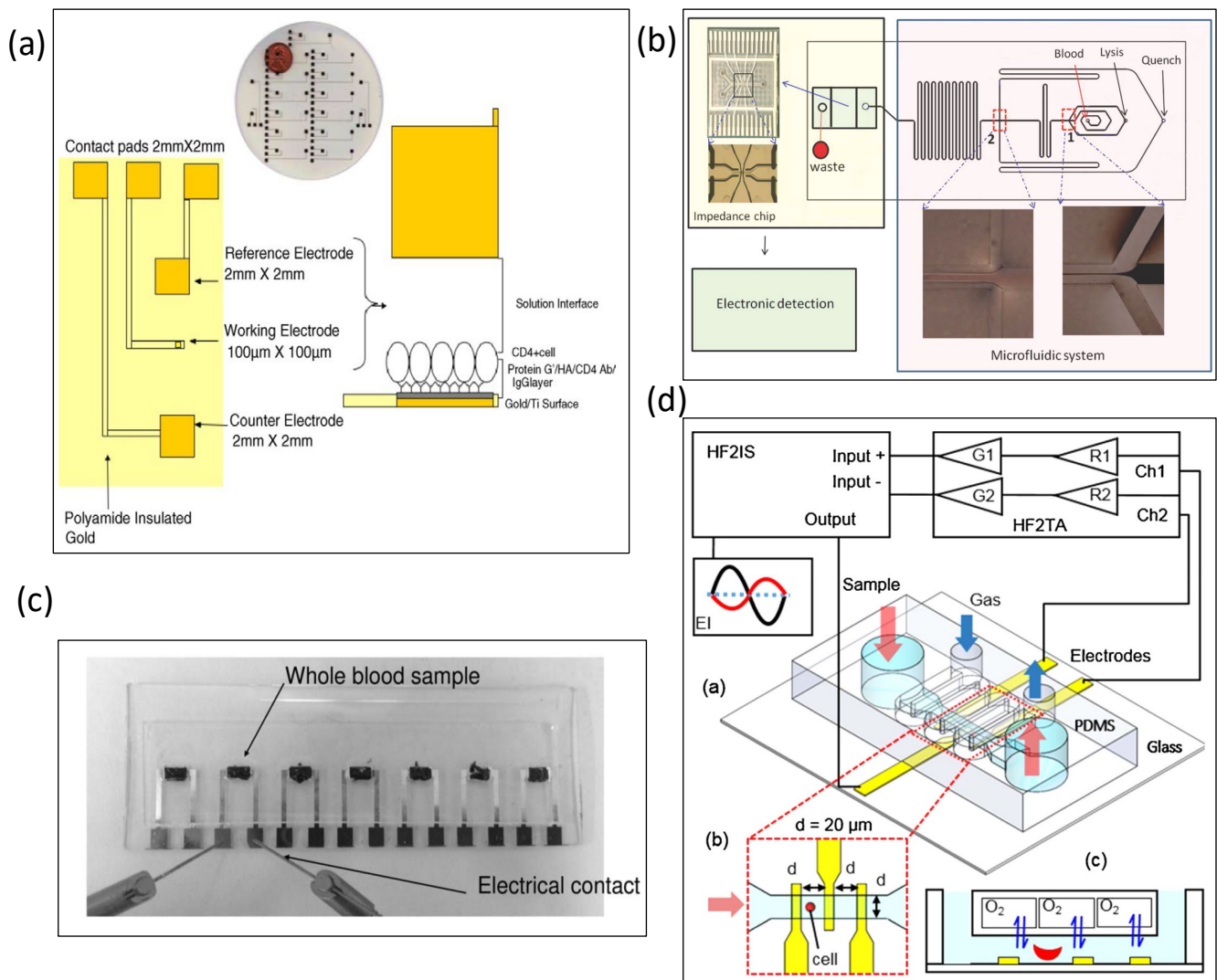


**Figure 5.** Glass-based impedance biosensors for detecting blood. (a) Three microelectrodes were used to sense the impedance of human CD4(+) cells in blood. Reproduced with permission from [61]. Copyright Biosensors and Bioelectronics 2005. (b) A microfluidic impedance cytometer was for red blood cell lysis. Reproduced with permission from [64]. Copyright Analytical Chemistry 2011. (c) A microfluidic chip was designed to detect electrical impedance for monitoring the blood coagulation process. Reproduced with permission from [65]. Copyright PLoS ONE 2013. (d) An electrical impedance microflow cytometer with controlled oxygen flow for the analysis of sickle blood cells. Reproduced with permission from [69]. Copyright Sensors and Actuators B: Chemical 2018.

### 5.3. Static Cell Analyzed by Electrical Impedance Spectroscopy

A microfluidic impedance sensor was designed to measure the cell migration of cancer cells in a three-dimensional extracellular matrix [70]. A total of 16 sets of sensing

electrode arrays and cell grabbing arrays were designed in the microchannel. Under continuous monitoring, the migration of MDA-MB-231 cells allowed for a rapid change in impedance amplitude (of about  $10 \Omega/s$ ). Liu et al. designed a microfluidic chip with embedded measurement electrodes to monitor the cell migration process using impedance measurement technology [71]. Cells were measured and recorded in the microfluidic channel as they pass through multiple parallel electrodes. This method enables the accurate and objective recording of cell migration activity and the calculation of migration rates among different stimulating drugs. Huang et al. designed a microchannel filled with Matrigel to quantify cell migration velocity as an assay tool, as shown in Figure 6a [72]. The successful measurement of cells suspended in a 3D environment and the induction of cell migration by stimulatory factors were used to record the migration speed of cells. The measurement sensitivity was better than that of a traditional trans-well assay.

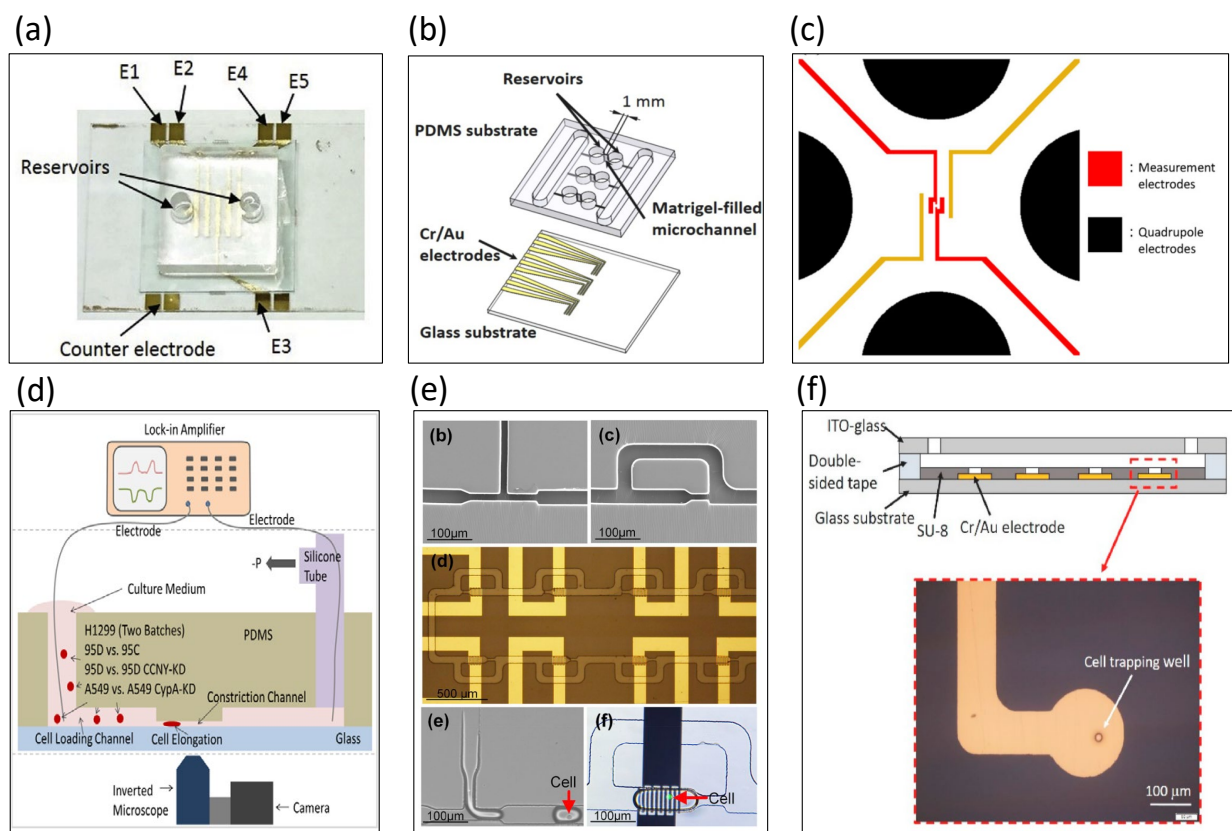


**Figure 6.** Static cell analyzed with electrical impedance spectroscopy. (a) A microchannel was designed filled with Matrigel to quantify cell migration velocity. Reproduced with permission from [72]. Copyright Analytica Chimica Acta 2020. (b) This chip was designed to induce angiogenesis to extend into the microchannel. Reproduced with permission from [73]. Copyright Sensors and Actuators B: Chemical 2022. (c) The relationship between the electrochemical impedance spectroscopy and withstand voltage was established with four different cells (HeLa, A549, MCF-7, and MDA-MB-231). Reproduced with permission from [74]. Copyright Sensors and Actuators B: Chemical 2012. (d) Because of the constriction of the microchannel, tumor cells, thus, are elongated for sensing impedance. Reproduced with permission from [75]. Copyright Biosensors and Bioelectronics 2014. (e) A microfluidic impedance sensing chip with droplets and microelectrode arrays was used to monitor the osteogenic differentiation of bone marrow mesenchymal stem cells. Reproduced with permission from [76]. Copyright Biosensors and Bioelectronics 2019. (f) Single stem cells were captured in a  $20 \mu\text{m}$  chamber by dielectrophoresis. Reproduced with permission from [77]. Copyright Talanta 2021.

Lei et al. developed a perfusion three-dimensional (3D) cell culture microfluidic chip combined with real-time and non-invasive impedance monitoring [73]. This device can simulate complex 3D biological microenvironments to culture cells and monitor the impedance changes under different concentrations of drug stimulation through impedance measurements. The impedance results are analyzed to determine the cell proliferation and chemosensitivity of 3D cell cultures. Lei et al. designed an impedance measurement device for cell colonies cultured on hydrogels [74–76]. Huang et al. constructed a 3D biological barrier using Matrigel and induced angiogenesis to extend into the microchannel, as shown in Figure 6b [77]. The angiogenesis process could be monitored by label-free impedance, using electrodes at the bottom of the microchannel. The device can also successfully quantify the time and distance of angiogenesis, thereby providing a reliable and quantitative method for the assay of angiogenesis.

Bieberich et al. developed electrical cell impedance spectroscopy to monitor the impedance response of PC12 and embryonic stem cells forming synapses [78]. Jang et al. published a study combining a cell capture method with microfabricated impedance spectroscopy [79], in which three micropillars were designed in the center of the microchannel to capture single HeLa cells. Cho et al. detailed the integrated microfluidic capture of single-cell technology with electrical impedance spectroscopy [80]. Hildebrandt et al. developed electrochemical impedance spectroscopy to distinguish the osteogenic differentiation of human mesenchymal stem cells [81]. In the application of cellular impedance to infectious parasites, Houssin et al. designed an electrochemical impedance spectroscopy approach to detect the presence of oocysts [82]. Dalmay et al. developed impedance spectroscopy to distinguish cancer stem cells and U87 glial cells (differentiated cells) [83]. The impedance spectrum designed by Bagnaninchi et al. can instantly monitor adipose stem cell (ADSC) differentiation [84]. Hong et al. established the relationship between electrochemical impedance spectroscopy and the withstand voltage of four different cells (HeLa, A549, MCF-7, and MDA-MB-231), as shown in Figure 6c [85]. Under a strong electric field, the cytoplasmic resistance decreases due to the opening of ion channels. The experimental results showed that different cells have not only different impedance spectra but also different withstand voltages. Chen et al. designed a microfluidic chip for capturing single cells and measuring impedance values [86]. Zhao et al. proposed to convert the measured impedance values into membrane capacitance (C-specific membrane) and cytoplasmic conductivity ( $\sigma$  cytoplasm), as shown in Figure 6d [87]. Due to the constriction of the microchannel, tumor cells become elongated. The experimental results demonstrated that tumor cells can be distinguished using two parameters: C-specific membrane and sigma cytoplasm. Ruan et al. integrated dielectrophoretic force and impedance sensors to detect lung circulating tumor cells [88]. Fan et al. designed a microfluidic impedance sensing chip with droplets and microelectrode arrays to monitor the osteogenic differentiation of bone marrow mesenchymal stem cells, as shown in Figure 6e [89]; the authors also proposed a model of cellular droplets. Lei et al. captured single stem cells in a 20  $\mu\text{m}$  chamber by dielectrophoresis, as shown in Figure 6f [90]; the cells were measured in the impedance spectrum range of 2–20 kHz.

#### 5.4. Dynamic Cell Analyzed by Microfluidic Impedance Cytometry

The development of microfluidic impedance flow cytometry is important for cell analysis. In this subsection, microfluidic impedance flow cytometry is divided into two parts for discussion: one is the principle of microfluidic impedance flow cytometry, and the other includes the sensing applications of microfluidic impedance flow cytometry.

Sun et al. designed two microfluidic impedance cytometers with parallel facing electrodes and coplanar electrodes [91]. For impedance measurements, parallel facing electrode designs are more sensitive than coplanar electrode designs. Holmes et al. used a microfabricated flow cytometer for the discrimination of micron-sized polymer beads [92]. Fluorescently labeled proteins were immobilized on the beads, which can be used to analyze the immune response. Negative dielectrophoretic force was used to focus the

polymer beads by the focusing electrodes. An electrical impedance flow cytometer for the high-speed analysis of particles was developed [93]. The impedance signal of polystyrene beads could be obtained in as little as 1 ms. Compared with microchannels fabricated by soft lithography, Kummrow et al. used ultraprecision milling technology to design 3D microchannels with horizontal and vertical focusing capabilities [94]. Fiber optics, mirrors, and electrodes were integrated into a flow cytometer for blood cells. Spencer et al. conducted a study on how the position of particles in a microchannel affects impedance measurements [95]. Impedance is related to the position of the particle in the vertical direction. A flow cytometer was designed by Barat et al. in order to measure both the optical and electrical properties of particles [96]. Daniel Spencer integrated optical fibers and waveguides into an impedance flow cytometer to measure electrical impedance (electrical volume and opacity), fluorescence, and large-angle side scatter without the need for particle focusing [97]. Haandbæk et al. published an article on microfabricated flow cytometry at high frequencies [98]. The experimental results indicated the ability at high frequencies to distinguish not only wild-type yeast and mutant strains but also opacity values at frequencies above 50 MHz.

David et al. used impedance flow cytometry to measure the viability and membrane potential of *Bacillus megaterium* cells [99]. A microfluidic impedance cytometer was designed for platelet analysis by Evander et al. [100], where the focusing electrodes allow for secondary focusing of the sample through the dielectrophoretic force. Lin et al. used a microfluidic impedance cytometer to detect quantified protein biomarkers [101]. For whole blood analysis, Simon et al. developed a microfabricated AC impedance cytometer with multi-frequency AC impedance and side scatter analysis capabilities [102]. Xie et al. proposed the concept of using a microfabricated impedance cytometer to detect electronic biomarkers [103]. By changing the dielectric properties of the particle, the authors designed a nanoelectronic barcode particle as an electronic biomarker. McGrath et al. used a microfluidic impedance flow cytometer to distinguish the oocysts of protozoan parasites, as shown in Figure 7a [104]. This chip can distinguish between *Cryptosporidium parvum*, *Cryptosporidium muris*, and *Giardia lamblia* within minutes. A microfluidic impedance cytometer integrating inertial focusing and liquid electrodes was developed for the high-throughput measurement of human breast tumor cells and leukocytes, as shown in Figure 7b [105]. The purpose of inertial focusing is to reduce cell adhesion and ensure that single cells pass through the sensing area. An interesting study involved the use of two microneedles, placed on either side of a microchannel to sense impedance values [106]. For clinical analysis and judgment, Sun et al. used multi-frequency impedance spectroscopy and machine learning to rapidly distinguish the survival of cancer cells under the action of anti-matriptase-conjugated drugs [107]. Sui et al. developed an impedance flow cytometer to detect spheroid green algae cells (*Picochlorum* SE3) at different salt concentrations, as shown in Figure 7c [108]. Mahesh et al. published a study on the observed “double-peak” characteristics of individual cells with high sensitivity to changes in cell membrane capacitance [109]. This phenomenon has limitations: it operates at the lower frequencies (400–800 kHz) of the beta-dispersion mechanism, and the microelectrodes must be coplanar and paired. The authors pointed out that changes in cell size and membrane capacitance can be resolved using a single frequency. A microfluidic impedance cytometer was used for the analysis of antigen-specific T lymphocytes, as shown in Figure 7d [110]. The experimental results demonstrated that differences in impedance can be observed among dead, healthy, and activated lymphocytes. Caselli et al. used artificial intelligence methods to decipher signals from microfluidic impedance cytometers [111]. The authors demonstrated two advances: (i) the use of a neural network to determine the dielectric properties of single cells in raw impedance data streams and (ii) resolving the impedance signatures of coincident cells. The results demonstrated that the neural network could increase the signal processing capability of the microfluidic impedance cytometer.

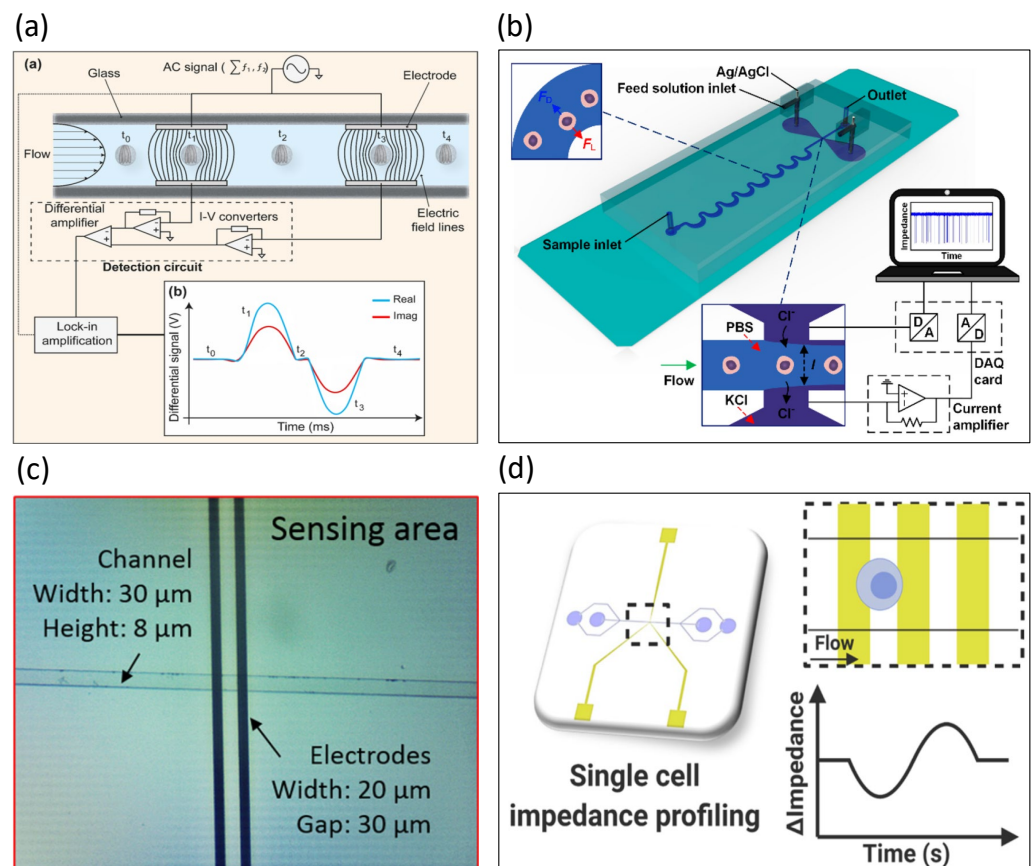


**Figure 7.** Dynamic cell analyzed by microfluidic impedance cytometry. (a) A model of the impedance flow cytometer was established to distinguish *Cryptosporidium parvum*, *Cryptosporidium muris*, and *Giardia lamblia* in minutes. Reproduced with permission from [104]. Copyright Scientific Reports 2017. (b) A microfluidic impedance cytometer integrating inertial focusing and liquid electrodes was developed. Reproduced with permission from [105]. Copyright Analytical Chemistry 2017. (c) An impedance flow cytometer was developed to detect spheroid green algae cells (*Picochlorum* SE3) at different salt concentrations. Reproduced with permission from [108]. Copyright Scientific Reports 2020. (d) A microfluidic impedance cytometer was used for the analysis of antigen-specific T lymphocytes. Reproduced with permission from [110]. Copyright Sensors and Actuators B: Chemical 2021.

### 5.5. Detection of Viruses

The key to the use of impedance biosensors for virus sensing is the immobilization of antibodies, where the antibody must be immobilized on the surface of the electrode first. However, the impedance signal will be altered due to the binding of both antibodies and antigens.

Pathogenic avian influenza viruses have been detected by impedance sensors [112]. The polyclonal antibody was immobilized on the surface of a gold microelectrode by protein A. The antibody–antigen binding reaction in the same research could be amplified by red blood cells, and the proposed impedance immunosensor could be completed in as little as 2 h. A portable impedance biosensor for avian influenza virus H5N2 was developed by Wang et al. [113]. Magnetic nanobeads and interdigitated array microelectrodes were integrated on a microfluidic chip, where the magnetic nanobeads captured avian influenza virus subtype-specific antibodies. The entire detection time was less than 1 h, which was greatly reduced compared with traditional avian influenza virus detection. The experimental results indicate that the sensitivity of the impedance biosensor is comparable to that of real-time reverse transcriptase PCR. Jacob Lum designed an impedance biosensor, mainly for avian influenza virus subtype H5N1 [55]. For this purpose, immunomagnetic

nanoparticles and interdigitated microelectrodes were designed on a microfluidic chip. The polyclonal antibody was immobilized on the surface of the microelectrode, which binds to avian influenza virus H5N1 to generate an impedance signal. Chicken red blood cells were used as biomarkers attached to interdigital microelectrodes. The results showed that the impedance signal can be increased by more than 100%. For the detection of human immunodeficiency virus, Shafiee et al. designed a microfluidic sensing chip to measure the impedance spectrum of virus nanolysates [114]. Two gold electrodes were designed on both sides of the microchannel cavity. The lysis of the virus results in the release of the ions and charged molecules of the virus into a non-ionic solution. That research demonstrated that impedance spectroscopy provides a convenient and rapid tool for the detection of multiple pathogens. Singh et al. developed an electrical impedance sensing chip to detect influenza H1N1 virus, as shown in Figure 8a [115,116], for which three microelectrodes were fabricated on a glass substrate. The authors used reduced graphene oxide and monoclonal antibodies as electrode modifications.

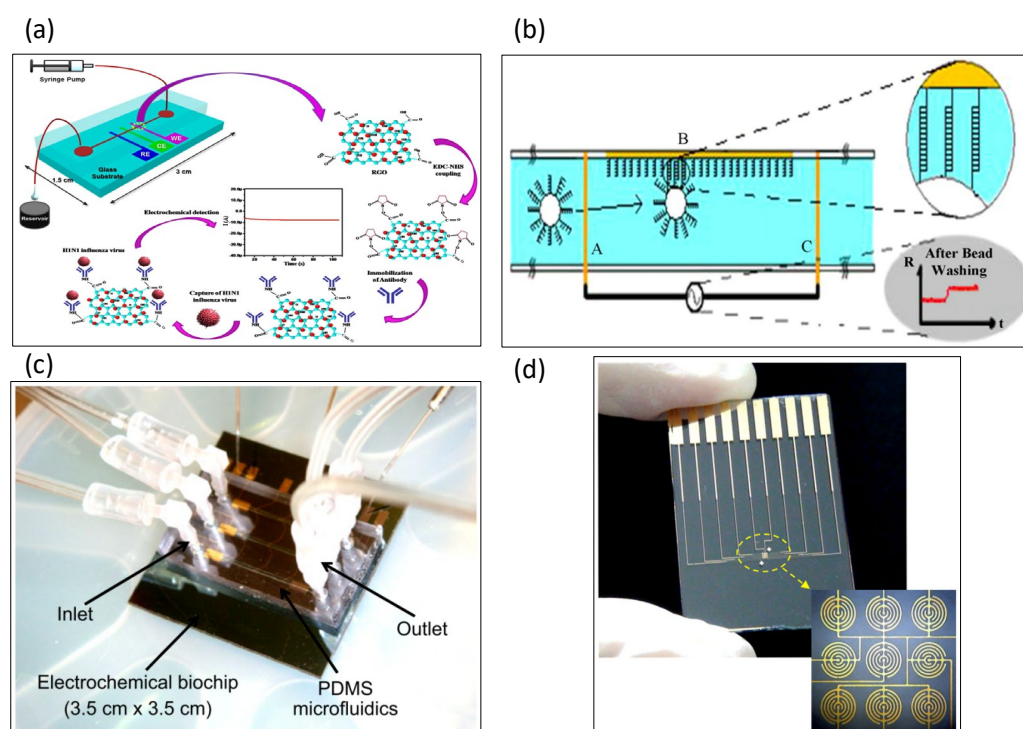


**Figure 8.** Glass-based impedance biosensors for detecting other organisms and chemicals. (a) An electrical impedance sensing chip was developed to detect influenza H1N1 virus. Reproduced with permission from [115]. Copyright Scientific Reports 2017. (b) Impedance sensors were developed for DNA hybridization. Reproduced with permission from [117]. Copyright Sensors and Actuators B: Chemical 2011. (c) Single-stranded DNA probes were functionalized onto electrodes. Complementary DNA hybridization was then induced using electrochemical impedance spectroscopy. Reproduced with permission from [118]. Copyright Biosensors and Bioelectronics 2012. (d) Galectin-1 protein is a biomarker of bladder cancer. An impedance immunosensor was developed to detect Galectin-1 protein in urine. The dielectrophoretic force was used to capture Galectin-1 antibody to improve the sensitivity of the sensor. Reproduced with permission from [119]. Copyright Biosensors and Bioelectronics 2016.

### 5.6. Detection of Other Analytes and Chemicals

Berdar et al. used an impedance sensor based on an interdigitated microelectrode array to sense DNA [116], for which 5  $\mu\text{m}$  wide microelectrodes were fabricated using a lift-off process method. The complementary probe was first immobilized on the electrode and hybridized to the target ssDNA. Finally, impedance sensors were used to detect the

pathogen *Salmonella choleraesuis* in dairy products. Javanmard et al. developed a set of impedance sensors for DNA hybridization, as shown in Figure 8b [117]. Oligonucleotide probes were immobilized on the surface of the microchannel, and target DNA strands were immobilized on the surface of polystyrene beads. Contact between the probe and the target DNA strand results in the hybridization of the DNA, leading to the capture of the polystyrene beads on the surface of the microchannel. An impedance chip for sensing DNA hybridization was developed by Hadar et al., as shown in Figure 8c [118]. Single-stranded DNA probes were functionalized onto electrodes, and complementary DNA hybridization was then induced using electrochemical impedance spectroscopy. DC-biased AC electro-osmotic vortex was utilized to design a label-free electrochemical impedance spectroscopy (EIS)-based DNA biosensing chip [119]. Based on the electro-osmotic vortex, 20-base target DNA fragments were hybridized to achieve 90% within 141 s. The ultrasensitive detection limit was 0.5 aM. Another study indicated that the electric field was manipulated by alternating current (AC) electrokinetics to improve hybridization efficiency and reduce hybridization time [120]. Thus, the chip was realized for faster and more efficient detection.

Galectin-1 protein is a biomarker of bladder cancer. An impedance immunosensor for detecting bladder cancer in urine was developed, as shown in Figure 8d [121]. Before measuring the impedance signal, the authors used dielectrophoretic force to capture nanoprobe (Gal-1 antibody) on the surface of the microelectrode, in order to improve the sensitivity of the sensor. Alsabbagh et al. designed a microfluidic impedance biosensor for the detection of myocardial infarction proteins by electrochemical impedance spectroscopy [122]; in particular, Troponin I, which is a biomarker for the diagnosis of myocardial infarction, was targeted. Self-assembled thiolated oligonucleotides tested on gold electrodes were found to perform better, as they improved the performance of the impedance signal. Fluorescence analysis and electrochemical impedance spectroscopy were integrated to measure aggregated C-reactive proteins [123]. The circular array of electrodes was designed to create electrokinetic flow for C-reactive protein aggregation. Interdigitated microelectrode arrays were modified by the self-assembled monolayers of mercaptocaproic acid for detecting the arthritis anti-CCP-ab biomarker [124]. The experimental results showed that the sensor response increased linearly with the stepwise increase of the biomarker concentration. A polyaniline (PANI)/MoS<sub>2</sub>-modified screen-printed electrode was detected for anti-cyclic citrullinated peptide [125]. Among them, the polymerized PANI-Au nanomatrix was utilized to entrap the aCCP antibodies for amplification of the higher signal. A peptide-based electrochemical sensor was used to detect autoantibodies for the diagnosis of rheumatoid arthritis [126]. The developed peptides were modified on the gold surface of the working electrode by a self-assembled monolayer method. Subsequently, the sensor was clinically demonstrated to have better sensitivity using 10 clinically validated samples from rheumatoid arthritis patients and 5 healthy control samples.

Chiriaco et al. designed a microfluidic electrochemical impedance biosensor to detect cholera toxin [127] with sensitivity less than 10 pM. Liu et al. developed a biosensor for the rapid screening of toxic substances in drinking water [128]. Cells are damaged due to toxins in water, resulting in decreased impedance and an increase in resonance frequency. Impedance and mass sensing measurements can help to improve sensor accuracy. An impedance biosensor was used to detect the cytotoxicity of tamoxifen in cervical cancer cells [129]. The experimental results showed that the dose of tamoxifen resulted in a significant reduction in the number of HeLa cells. The same article demonstrated that impedance biosensors can be used for the evaluation of novel drugs and cytotoxicity.

A microfluidic impedance sensor was designed for pesticide detection in vegetables [130]. Anti-chlorpyrifos monoclonal antibody was immobilized on an interdigitated electrode array. The capture of chlorpyrifos produced a change in impedance. Zeng et al. integrated magnetic focusing into impedance microsensors for oil monitoring [131]. The highly focused magnetic field was derived from two electromagnetic coils and eight silicon steel tips, where the silicon steel tips greatly improved the sensitivity of the sensor.

### 5.7. Conclusions of the Glass Chips

Microfluidic impedance sensor glass chips have two great development directions: electrochemical impedance spectroscopy and electrical impedance flow cytometry. The difference between the two lies in the state of the measured object. For example, in an electrical impedance flow cytometer, as shown in Figure 6, the cells are stationary. The cells may be attached to the bottom of a microgroove or a microchamber, where the culture medium is quiescent. On the other hand, cells may be trapped by the microstructures and focused by the dielectrophoretic force, thus, fixing them in one position. In an electrical impedance flow cytometer, the cells are in a dynamic state, as shown in Figure 7. For the impedance sensing of other organisms, the main technology relies on the modification of electrodes and the combination of antigens and antibodies.

## 6. Paper-Based Impedance Biosensors

Lei et al. combined the electrical impedance measurement technique with the hydrophilic properties of a paper base into a system for recording and analysis [132]. Through impedance analysis, a trend proportional to cell proliferation was observed. A paper-based electrochemical impedance DNA sensor for tuberculosis detection was developed by Teengam et al., as shown in Figure 9a [133]. Carbon graphene inks were printed as working and counter electrodes, while reference electrodes and conductive pads were screen-printed with silver/silver chloride ink. Pyrrolidine peptide nucleic acid (acpcPNA) was immobilized on cellulose paper, and changes in impedance were induced in the presence of *Mycobacterium tuberculosis*. Rengaraj et al. developed paper-based electrodes for the impedance detection of bacteria in water, as shown in Figure 9b [134]. The paper-based electrodes were made of carbon on hydrophobic paper formed by screen printing. The cellulose was cross-linked before use in order to enhance the strength of the paper substrate and the electrical properties of the screen-printed electrodes. The same article was the first to combine the hydrophobicity of paper substrates with the electrochemical functionalization of electrodes. A paper-based microfluidic impedance chip was developed to sense alpha-fetoprotein in human serum using peptide-modified plastic paper [135]. The sensor included two layers, where the upper layer was cellulose chromatography paper, and the lower layer was plastic paper. Among them, the sensing electrodes were printed with Ag-20 wt % graphene. The limit value of alpha-fetoprotein in PBS detected by the sensor was 1 ng/mL. Lei et al. used hydrogel to encapsulate cells and then cultured them on top of paper substrates [136]. The resulting analysis could more accurately distinguish the impedance differences between two cells and under the action of a drug. Some studies have used electrochemical impedance spectroscopy to detect miRNA-34a, which is a biomarker of cancer and Alzheimer's disease [137]. PAMAM dendrimers were modified on the surface of screen-printed electrodes. The results indicated that the difference between miRNA-34a and miRNA-15 or miRNA-660 could be distinguished through electrochemical impedance spectroscopy. Cardiac troponin I is a biomarker for the early diagnosis of acute myocardial infarction. A paper-based impedance immunosensor was developed to detect cardiac troponin I [138], for which multi-walled carbon nanotubes were immobilized on carbon ink electrodes. Then, cardiac troponin I antibody was immobilized on multi-walled carbon nanotubes. Finally, cardiac troponin I was captured by the antibody, affecting the impedance signal. Li et al. designed paper-based electrochemical impedance spectroscopy to detect coronavirus (COVID-19), as shown in Figure 9c [139]. The carbon ink was first printed on paper, and a layer of zinc oxide nanowires was grown on the carbon ink. Then, probes and blocking molecules were immobilized on its surface. Finally, the target molecules were captured for impedance sensing. The results showed that the enhanced ZnO nanowires can improve impedance sensitivity. Electrochemical impedance spectroscopy was used to analyze artificial sweat using hand-painted electrodes [140]. Electrodes were drawn on the opposite side of the paper in order to reduce the double-layer capacitance. The silver electrode pattern paper chip had stronger impedance stability than the graphite electrode paper chip. Research and development of paper-based electrochemical impedance spectroscopy

was conducted for the detection of microRNA 155 [141], for which gold nanoparticles changed the properties of paper-based electrodes. S. Karupiah developed a paper-based impedance biosensor for monitoring bacteria in water [142]. The electrodes of the biosensor were screen-printed with graphene (G) and then surface-modified with graphene oxide (GO). The lectin concanavalin A was then immobilized on the modified electrode described above. A paper-based impedance sensor was used to sense miRNA-155 and miRNA-21 for the early diagnosis of lung cancer, as shown in Figure 9d [143]. The authors used MoS<sub>2</sub> crystals and MoS<sub>2</sub> nanosheets to modify the paper-based electrodes. Paper-based electrochemical impedance spectroscopy was used to detect foodborne pathogens (*Listeria*) [144]. Tungsten disulfide nanostructures were used as paper-based electrodes for impedance sensors.

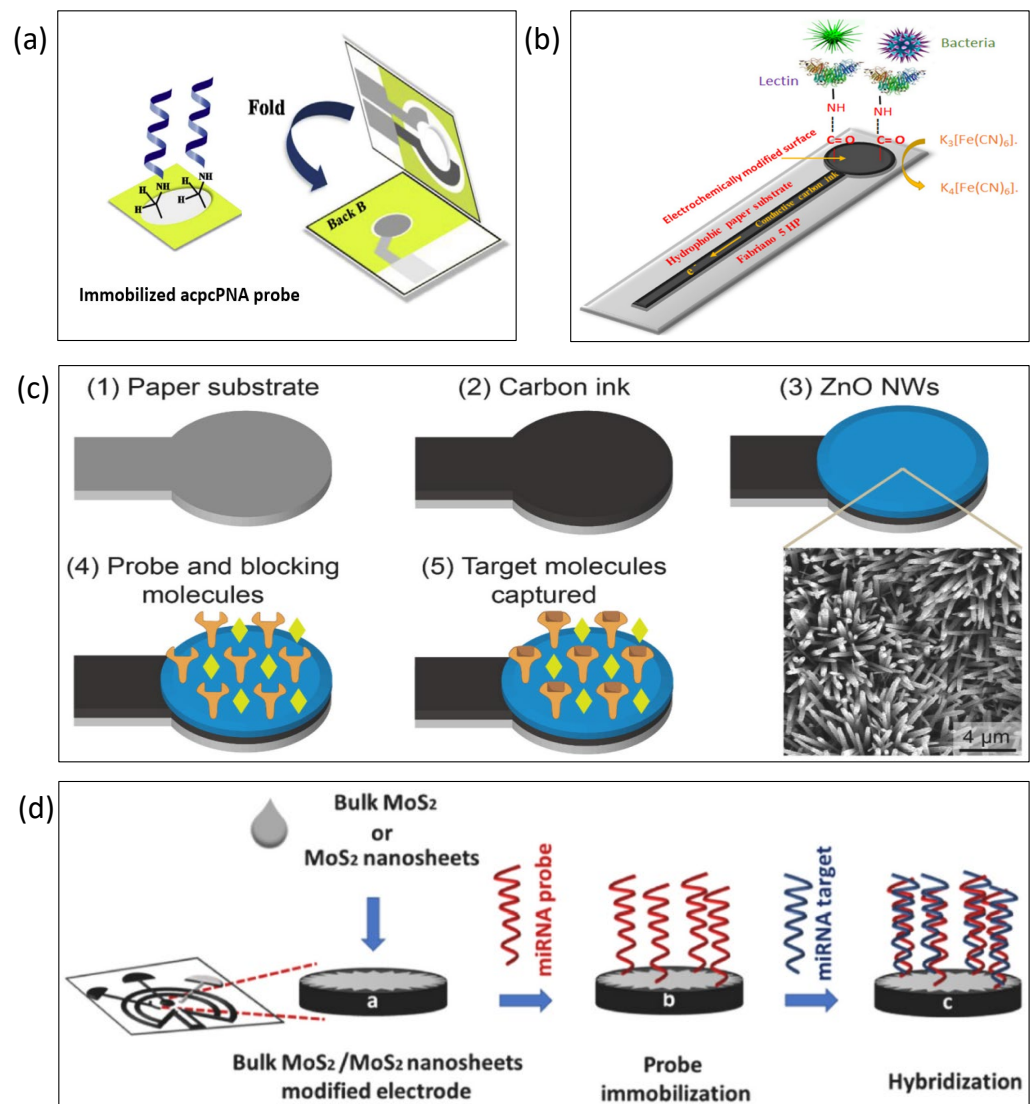


**Figure 9.** Paper-based impedance biosensors. (a) A paper-based electrochemical impedance DNA sensor was developed for tuberculosis detection. Reproduced with permission from [133]. Copyright Analytica Chimica Acta 2018. (b) Paper-based electrodes for impedance sensors were used to detect the bacteria in water. Reproduced with permission from [134]. Copyright Sensors and Actuators B: Chemical 2018. (c) A paper-based electrochemical impedance spectroscopy was designed to detect coronavirus (COVID-19). Reproduced with permission from [139]. Copyright Biosensors and Bioelectronics 2021. (d) Paper-based impedance sensor was used to sense miRNA-155 and miRNA-21 for early diagnosis of lung cancer. Reproduced with permission from [143]. Copyright Talanta 2022.

Paper-based chips have great advantages due to their low material cost. Microelectrodes with small line widths on paper-based chips and antibodies combined onto the microelectrodes will be key technologies for the development of paper-based chips.

## 7. Stretchable Biosensors

Furniturewalla et al. designed a microfluidic impedance cytometer on a flexible circuit board in the form of a portable wristband [145]. Lock-in amplification, a microfluidic biosensor, a microcontroller, and a Bluetooth module are integrated into the wristband. Flexible and stretchable biosensors for skin physiological parameter monitoring have been developed [146], where screen printing was used to fabricate sensing electrodes in flexible and stretchable conductive materials originally intended for epidermal tattooing. A retractable body biosensor for sensing the biomarker cortisol in sweat was published, as shown in Figure 10a [147]. A pullable body impedance biosensor was designed at the bottom layer and attached to the skin, following which microfluidic microvalves and microchannels were applied to this wearable patch. A stretchable microfluidic immunobiosensor patch was used for sensing neuropeptide Y in human sweat [148]. Conductive microfibers that can be stretched help to improve the sensitivity of the biosensor patches. Sensors attached to the skin can detect biomarker concentrations in human sweat at levels as low as fm. A wearable microfluidic impedance immunosensor for sweat cortisol detection was designed, as shown in Figure 10b [149], where microfluidic channels and chambers were integrated into the wearable patch, and Ti3C2Tx MXene nanosheets were incorporated in the porous structure of graphene. The wearable microfluidic impedance immunosensor could detect cortisol down to 88 pM.

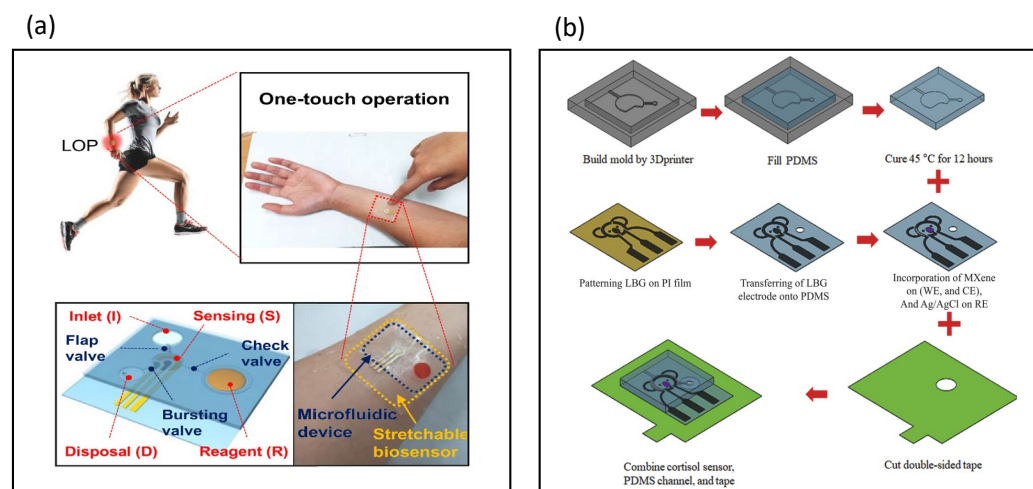


**Figure 10.** Stretchable impedance biosensors. (a) All-polymer electrochemical microfluidic biosensors were used for sensing the biomarker cortisol in sweat. The pullable body impedance biosensor was designed at the bottom layer and attached to the skin. Reproduced with permission from [147]. Copyright Biosensors and Bioelectronics 2020. (b) A wearable microfluidic impedance immunosensor was designed for sweat cortisol detection. Microfluidic channels and chambers were integrated into the wearable patch. Reproduced with permission from [149]. Copyright Sensors and Actuators B: Chemical 2021.

Stretchable chips for microfluidic impedance sensors comprise a novel research direction. At present, impedance sensing signals are mostly measured on the skin. The stretchability and bendability of such materials are key features, especially the flexibility of the electrode materials. In this line, conductive hydrogels may be a helpful technology.

## 8. Conclusions

Impedance biosensors integrated with microfluidic technology are powerful tools for understanding electrical information in microscopic and sub-microscopic organisms. The integrated sensors have the key characteristics of improved sensitivity, reduced reagent consumption, short analysis time, reduced instrument size, and simple operation. In this paper, the developed microfluidic impedance sensors were classified into six categories: silicon chip-, PCB chip-, polymer chip-, glass chip-, paper chip-, and stretchable chip-based. No matter which type of chip is to be developed, the microfabrication of microelectrodes and the bonding of chemicals are key technologies.

Silicon-based chips are made by the MEMS process developed by Taiwan Semiconductor Manufacturing Co., Ltd., which can become the commercialization direction of electrical impedance biosensors. The development of PCB chips was limited by the line width of the electrodes, which makes it impossible to improve sensitivity. Therefore, PCB chips are more suitable for production or commercial designs with a fast sensing speed and low sensitivity requirements. Polymer materials are suitable for mass production. Therefore, polymer chips can be one of the options for commercialization. Microfluidic impedance sensor glass chips have two great development directions: electrochemical impedance spectroscopy and electrical impedance flow cytometry. The difference between the two lies in the state of the measured object. In an electrical impedance flow cytometer, the cells are stationary. In an electrical impedance flow cytometer, the cells are in a dynamic state. For the impedance sensing of other organisms, the main technology relies on the modification of electrodes and the combination of antigens and antibodies.

Since the development of microfluidic impedance sensors, the development of the principle has mostly stagnated since 2014, especially electrical impedance flow cytometers. Therefore, with regard to the development of sensing applications, specific antigen–antibody binding may not easily become a break-point in relevant research. Instead, paper-based chips and stretchable chips are expected to become the focus of future development related to microfluidic impedance sensors. As the COVID-19 virus has spread globally in recent years, this variable virus needs to be sensed by electrical impedance biosensors.

**Author Contributions:** Writing—original draft preparation, Y.-S.C. and C.-H.H.; writing—review and editing, P.-C.P., J.S. and K.F.L.; funding acquisition, J.S. and K.F.L. All authors have read and agreed to the published version of the manuscript.

**Funding:** This work was supported by the National Science and Technology Council, Taiwan (Project No. MOST111-2221-E-182-006-MY3) and the National Research Foundation of Korea (NRF) grant funded by the Korean Government (MSIT) (Project No. 2022R1A2C4001652).

**Institutional Review Board Statement:** Not applicable.

**Informed Consent Statement:** Not applicable.

**Data Availability Statement:** Not applicable.

**Conflicts of Interest:** The authors declare no conflict of interest.

## References

1. Kim, S.; Song, H.; Ahn, H.; Kim, T.; Jung, J.; Cho, S.K.; Shin, D.M.; Choi, J.R.; Hwang, Y.H.; Kim, K. A Review of Advanced Impedance Biosensors with Microfluidic Chips for Single-Cell Analysis. *Biosensors* **2021**, *11*, 412. [\[CrossRef\]](#)
2. Ayliffe, H.E.; Frazier, A.B.; Rabbitt, R.D. Electric impedance spectroscopy using microchannels with integrated metal electrodes. *J. Microelectromech. Syst.* **1999**, *8*, 50–57. [\[CrossRef\]](#)
3. Zhang, Z.; Huang, X.W.; Liu, K.; Lan, T.C.; Wang, Z.X.; Zhu, Z. Recent Advances in Electrical Impedance Sensing Technology for Single-Cell Analysis. *Biosensors* **2021**, *11*, 470. [\[CrossRef\]](#)
4. Lei, K.F. Review on Impedance Detection of Cellular Responses in Micro/Nano Environment. *Micromachines* **2014**, *5*, 1–12. [\[CrossRef\]](#)
5. Giaever, I.; Keese, C.R. Monitoring fibroblast behavior in tissue culture with an applied electric field. *Proc. Natl. Acad. Sci. USA* **1984**, *81*, 3761–3764. [\[CrossRef\]](#)

6. Giaever, I.; Keese, C.R. Use of electric fields to monitor the dynamical aspect of cell behavior in tissue culture. *IEEE Trans. Biomed. Eng.* **1986**, *33*, 242–247. [[CrossRef](#)]
7. Giaever, I.; Keese, C.R. Micromotion of mammalian-cells measured electrically. *Proc. Natl. Acad. Sci. USA* **1991**, *88*, 7896–7900. [[CrossRef](#)]
8. Giaever, I.; Keese, C.R. A morphological biosensor for mammalian-cells. *Nature* **1993**, *366*, 591–592. [[CrossRef](#)]
9. Grossi, M.; Riccò, B. Electrical impedance spectroscopy (EIS) for biological analysis and food characterization: A review. *J. Sens. Sens. Syst.* **2017**, *6*, 303–325. [[CrossRef](#)]
10. Sun, T.; Bernabini, C.; Morgan, H. Single-Colloidal Particle Impedance Spectroscopy: Complete Equivalent Circuit Analysis of Polyelectrolyte Microcapsules. *Langmuir* **2010**, *26*, 3821–3828. [[CrossRef](#)]
11. Kamensky, L.A.; Melamed, M.R.; Derman, H. Spectrophotometer: New instrument for ultrarapid cell analysis. *Science* **1965**, *150*, 630–631. [[CrossRef](#)] [[PubMed](#)]
12. Gawad, S.; Schild, L.; Renaud, P. Micromachined impedance spectroscopy flow cytometer for cell analysis and particle sizing. *Lab Chip* **2001**, *1*, 76–82. [[CrossRef](#)]
13. Gawad, S.; Cheung, K.; Seger, U.; Bertsch, A.; Renaud, P. Dielectric spectroscopy in a micromachined flow cytometer: Theoretical and practical considerations. *Lab Chip* **2004**, *4*, 241–251. [[CrossRef](#)] [[PubMed](#)]
14. Cheung, K.; Gawad, S.; Renaud, P. Impedance spectroscopy flow cytometry: On-chip label-free cell differentiation. *Cytom. Part A* **2005**, *65A*, 124–132. [[CrossRef](#)] [[PubMed](#)]
15. Hoffman, R.A.; Johnson, T.S.; Britt, W.B. Flow cytometric electronic direct current volume and radiofrequency impedance measurements of single cells and particles. *Cytometry* **1981**, *1*, 377–384. [[CrossRef](#)]
16. Sun, T.; Morgan, H. Single-cell microfluidic impedance cytometry: A review. *Microfluid. Nanofluid.* **2010**, *8*, 423–443. [[CrossRef](#)]
17. Van Gerwen, P.; Laureyn, W.; Laureys, W.; Huyberechts, G.; De Beeck, M.O.; Baert, K.; Suls, J.; Sansen, W.; Jacobs, P.; Hermans, L.; et al. Nanoscaled interdigitated electrode arrays for biochemical sensors. *Sens. Actuator B Chem.* **1998**, *49*, 73–80. [[CrossRef](#)]
18. Gomez, R.; Bashir, R.; Sarikaya, A.; Ladisch, M.R.; Sturgis, J.; Robinson, J.P.; Geng, T.; Bhunia, A.K.; Apple, H.L.; Wereley, S. Microfluidic Biochip for Impedance Spectroscopy of Biological Species. *Biomed. Microdevices* **2001**, *3*, 201–209. [[CrossRef](#)]
19. Radke, S.M.; Alocilja, E.C. Design and fabrication of a microimpedance biosensor for bacterial detection. *IEEE Sens. J.* **2004**, *4*, 434–440. [[CrossRef](#)]
20. Radke, S.M.; Alocilja, E.C. A microfabricated biosensor for detecting foodborne bioterrorism agents. *IEEE Sens. J.* **2005**, *5*, 744–750. [[CrossRef](#)]
21. Hong, J.; Yoon, D.S.; Kim, S.K.; Kim, T.S.; Kim, S.; Pak, E.Y.; No, K. AC frequency characteristics of coplanar impedance sensors as design parameters. *Lab Chip* **2005**, *5*, 270–279. [[CrossRef](#)]
22. Kloss, D.; Fischer, M.; Rothmel, A.; Simon, J.C.; Robitzki, A.A. Drug testing on 3D in vitro tissues trapped on a microcavity chip. *Lab Chip* **2008**, *8*, 879–884. [[CrossRef](#)]
23. James, C.D.; Reuel, N.; Lee, E.S.; Davalos, R.V.; Mani, S.S.; Carroll-Portillo, A.; Rebeil, R.; Martino, A.; Apblett, C.A. Impedimetric and optical interrogation of single cells in a microfluidic device for real-time viability and chemical response assessment. *Biosens. Bioelectron.* **2008**, *23*, 845–851. [[CrossRef](#)]
24. Singh, K.V.; Whited, A.M.; Rugineni, Y.; Barrett, T.W.; King, J.; Solanki, R. 3D nanogap interdigitated electrode array biosensors. *Anal. Bioanal. Chem.* **2010**, *397*, 1493–1502. [[CrossRef](#)]
25. Arya, S.K.; Chornokur, G.; Venugopal, M.; Bhansali, S. Antibody functionalized interdigitated mu-electrode (ID mu E) based impedimetric cortisol biosensor. *Analyst* **2010**, *135*, 1941–1946. [[CrossRef](#)]
26. Chen, Y.; Wong, C.C.; Pui, T.S.; Nadipalli, R.; Weerasekera, R.; Chandran, J.; Yu, H.; Rahman, A.R.A. CMOS high density electrical impedance biosensor array for tumor cell detection. *Sens. Actuator B Chem.* **2012**, *173*, 903–907. [[CrossRef](#)]
27. Ma, H.B.; Wallbank, R.W.R.; Chaji, R.; Li, J.H.; Suzuki, Y.; Jiggins, C.; Nathan, A. An impedance-based integrated biosensor for suspended DNA characterization. *Sci. Rep.* **2013**, *3*, 7. [[CrossRef](#)]
28. Cunci, L.; Vargas, M.M.; Cunci, R.; Gomez-Moreno, R.; Perez, I.; Baerga-Ortiz, A.; Gonzalez, C.I.; Cabrera, C.R. Real-time detection of telomerase activity in cancer cells using a label-free electrochemical impedimetric biosensing microchip. *RSC Adv.* **2014**, *4*, 52357–52365. [[CrossRef](#)]
29. Shin, K.S.; Ji, J.H.; Hwang, K.S.; Jun, S.C.; Kang, J.Y. Sensitivity Enhancement of Bead-based Electrochemical Impedance Spectroscopy (BEIS) biosensor by electric field-focusing in microwells. *Biosens. Bioelectron.* **2016**, *85*, 16–24. [[CrossRef](#)]
30. Pursey, J.P.; Chen, Y.; Stulz, E.; Park, M.K.; Kongsuphol, P. Microfluidic electrochemical multiplex detection of bladder cancer DNA markers. *Sens. Actuator B Chem.* **2017**, *251*, 34–39. [[CrossRef](#)]
31. Brosel-Oliu, S.; Mergel, O.; Uria, N.; Abramova, N.; van Rijn, P.; Bratov, A. 3D impedimetric sensors as a tool for monitoring bacterial response to antibiotics. *Lab Chip* **2019**, *19*, 1436–1447. [[CrossRef](#)] [[PubMed](#)]
32. Pan, Y.X.; Jiang, D.M.; Gu, C.L.; Qiu, Y.; Wan, H.; Wang, P. 3D microgroove electrical impedance sensing to examine 3D cell cultures for antineoplastic drug assessment. *Microsyst. Nanoeng.* **2020**, *6*, 10. [[CrossRef](#)] [[PubMed](#)]
33. Hsiao, Y.P.; Mukundan, A.; Chen, W.C.; Wu, M.T.; Hsieh, S.C.; Wang, H.C. Design of a Lab-On-Chip for Cancer Cell Detection through Impedance and Photoelectrochemical Response Analysis. *Biosensors* **2022**, *12*, 405. [[CrossRef](#)] [[PubMed](#)]
34. Valekunja, R.B.; Kamakoti, V.; Peter, A.; Phadnis, S.; Prasad, S.; Nagaraj, V.J. The detection of papaya ringspot virus coat protein using an electrochemical immunosensor. *Anal. Methods* **2016**, *8*, 8534–8541. [[CrossRef](#)]

35. Jin, S.R.; Ye, Z.Z.; Wang, Y.X.; Ying, Y.B. A Novel Impedimetric Microfluidic Analysis System for Transgenic Protein Cry1Ab Detection. *Sci. Rep.* **2017**, *7*, 8. [[CrossRef](#)] [[PubMed](#)]
36. Chang, Y.J.; Ho, C.Y.; Zhou, X.M.; Yen, H.R. Determination of degree of RBC agglutination for blood typing using a small quantity of blood sample in a microfluidic system. *Biosens. Bioelectron.* **2018**, *102*, 234–241. [[CrossRef](#)]
37. Fuentes-Velez, S.; Fagoonee, S.; Sanginario, A.; Pizzi, M.; Altruda, F.; Demarchi, D. Electrical Impedance-Based Characterization of Hepatic Tissue with Early-Stage Fibrosis. *Biosensors* **2022**, *12*, 116. [[CrossRef](#)]
38. Zou, Z.W.; Kai, J.H.; Rust, M.J.; Han, J.; Ahn, C.H. Functionalized nano interdigitated electrodes arrays on polymer with integrated microfluidics for direct bio-affinity sensing using impedimetric measurement. *Sens. Actuator A Phys.* **2007**, *136*, 518–526. [[CrossRef](#)]
39. Sabounchi, P.; Morales, A.M.; Ponce, P.; Lee, L.P.; Simmons, B.A.; Davalos, R.V. Sample concentration and impedance detection on a microfluidic polymer chip. *Biomed. Microdevices* **2008**, *10*, 661–670. [[CrossRef](#)]
40. Dapra, J.; Lauridsen, L.H.; Nielsen, A.T.; Rozlosnik, N. Comparative study on aptamers as recognition elements for antibiotics in a label-free all-polymer biosensor. *Biosens. Bioelectron.* **2013**, *43*, 315–320. [[CrossRef](#)]
41. Pires, L.; Sachsenheimer, K.; Kleintschek, T.; Waldbaur, A.; Schwartz, T.; Rapp, B.E. Online monitoring of biofilm growth and activity using a combined multi-channel impedimetric and amperometric sensor. *Biosens. Bioelectron.* **2013**, *47*, 157–163. [[CrossRef](#)] [[PubMed](#)]
42. Rosati, G.; Dapra, J.; Cherre, S.; Rozlosnik, N. Performance Improvement by Layout Designs of Conductive Polymer Microelectrode Based Impedimetric Biosensors. *Electroanalysis* **2014**, *26*, 1400–1408. [[CrossRef](#)]
43. Shi, Z.Z.; Tian, Y.L.; Wu, X.S.; Li, C.M.; Yu, L. A one-piece lateral flow impedimetric test strip for label-free clenbuterol detection. *Anal. Methods* **2015**, *7*, 4957–4964. [[CrossRef](#)]
44. Sharif, S.; Wang, Y.X.; Ye, Z.Z.; Wang, Z.; Qiu, Q.M.; Ying, S.N.; Ying, Y.B. A novel impedimetric sensor for detecting LAMP amplicons of pathogenic DNA based on magnetic separation. *Sens. Actuator B Chem.* **2019**, *301*, 6. [[CrossRef](#)]
45. Lakey, A.; Ali, Z.; Scott, S.M.; Chebil, S.; Korri-Youssoufi, H.; Hunor, S.; Ohlander, A.; Kuphal, M.; Marti, J.S. Impedimetric array in polymer microfluidic cartridge for low cost point-of-care diagnostics. *Biosens. Bioelectron.* **2019**, *129*, 147–154. [[CrossRef](#)]
46. Ma, W.R.; Liu, L.L.; Xu, Y.; Wang, L.; Chen, L.; Yan, S.; Shui, L.L.; Wang, Z.J.; Li, S.B. A highly efficient preconcentration route for rapid and sensitive detection of endotoxin based on an electrochemical biosensor. *Analyst* **2020**, *145*, 4204–4211. [[CrossRef](#)]
47. Niaraki, A.; Shirsavar, M.A.; Aykar, S.S.; Taghavimehr, M.; Montazami, R.; Hashemi, N.N. Minute-sensitive real-time monitoring of neural cells through printed graphene microelectrodes. *Biosens. Bioelectron.* **2022**, *210*, 8. [[CrossRef](#)]
48. Chmayssem, A.; Tanase, C.E.; Verplanck, N.; Gougis, M.; Mourier, V.; Zebda, A.; Ghaemmaghami, A.M.; Mailley, P. New Microfluidic System for Electrochemical Impedance Spectroscopy Assessment of Cell Culture Performance: Design and Development of New Electrode Material. *Biosensors* **2022**, *12*, 452. [[CrossRef](#)]
49. Hantschke, M.; Triantis, I.F. Optimisation of an Electrical Impedance Sensor for Use in Microfluidic Chip Electrophoresis. *IEEE Sens. J.* **2022**, *22*, 16–24. [[CrossRef](#)]
50. Ruan, C.M.; Yang, L.J.; Li, Y.B. Immunobiosensor chips for detection of Escherichia coli O157:H7 using electrochemical impedance spectroscopy. *Anal. Chem.* **2002**, *74*, 4814–4820. [[CrossRef](#)]
51. Yang, L.J.; Li, Y.B.; Griffis, C.L.; Johnson, M.G. Interdigitated microelectrode (IME) impedance sensor for the detection of viable Salmonella typhimurium. *Biosens. Bioelectron.* **2004**, *19*, 1139–1147. [[CrossRef](#)]
52. Yang, L.J.; Li, Y.B.; Erf, G.F. Interdigitated array microelectrode-based electrochemical impedance immunosensor for detection of Escherichia coli O157:H7. *Anal. Chem.* **2004**, *76*, 1107–1113. [[CrossRef](#)] [[PubMed](#)]
53. Wang, R.H.; Ruan, C.M.; Kanayeva, D.; Lassiter, K.; Li, Y.B. TiO<sub>2</sub> nanowire bundle microelectrode based impedance immunosensor for rapid and sensitive detection of Listeria monocytogenes. *Nano Lett.* **2008**, *8*, 2625–2631. [[CrossRef](#)] [[PubMed](#)]
54. Tan, F.; Leung, P.H.M.; Liu, Z.B.; Zhang, Y.; Xiao, L.D.; Ye, W.W.; Zhang, X.; Yi, L.; Yang, M. A PDMS microfluidic impedance immunosensor for *E. coli* O157:H7 and *Staphylococcus aureus* detection via antibody-immobilized nanoporous membrane. *Sens. Actuator B Chem.* **2011**, *159*, 328–335. [[CrossRef](#)]
55. Lum, J.; Wang, R.H.; Lassiter, K.; Srinivasan, B.; Abi-Ghanem, D.; Berghman, L.; Hargis, B.; Tung, S.; Lu, H.G.; Li, Y.B. Rapid detection of avian influenza H5N1 virus using impedance measurement of immuno-reaction coupled with RBC amplification. *Biosens. Bioelectron.* **2012**, *38*, 67–73. [[CrossRef](#)]
56. Dastider, S.G.; Barizuddin, S.; Dweik, M.; Almasri, M. A micromachined impedance biosensor for accurate and rapid detection of *E. coli* O157:H7. *RSC Adv.* **2013**, *3*, 26297–26306. [[CrossRef](#)]
57. Couniot, N.; Vanzielegem, T.; Rasson, J.; Van Overstraeten-Schlogel, N.; Poncelet, O.; Mahillon, J.; Francis, L.A.; Flandre, D. Lytic enzymes as selectivity means for label-free, microfluidic and impedimetric detection of whole-cell bacteria using ALD-Al<sub>2</sub>O<sub>3</sub> passivated microelectrodes. *Biosens. Bioelectron.* **2015**, *67*, 154–161. [[CrossRef](#)]
58. Liu, J.Y.; Jasim, I.; Abdullah, A.; Shen, Z.Y.; Zhao, L.; El-Dweik, M.; Zhang, S.P.; Almasri, M. An integrated impedance biosensor platform for detection of pathogens in poultry products. *Sci. Rep.* **2018**, *8*, 10. [[CrossRef](#)] [[PubMed](#)]
59. Dastider, S.G.; Abdullah, A.; Jasim, I.; Yuksek, N.S.; Dweik, M.; Almasri, M. Low concentration *E. coli* O157:H7 bacteria sensing using microfluidic MEMS biosensor. *Rev. Sci. Instrum.* **2018**, *89*, 9. [[CrossRef](#)]
60. Liu, J.Y.; Jasim, I.; Shen, Z.Y.; Zhao, L.; Dweik, M.; Zhang, S.P.; Almasri, M. A microfluidic based biosensor for rapid detection of *Salmonella* in food products. *PLoS ONE* **2019**, *14*, e0216873. [[CrossRef](#)]

61. Mishra, N.N.; Retterer, S.; Zieziulewicz, T.J.; Isaacson, M.; Szarowski, D.; Mousseau, D.E.; Lawrence, D.A.; Turner, J.N. On-chip micro-biosensor for the detection of human CD4(+) cells based on AC impedance and optical analysis. *Biosens. Bioelectron.* **2005**, *21*, 696–704. [[CrossRef](#)] [[PubMed](#)]
62. Kuttel, C.; Nascimento, E.; Demierre, N.; Silva, T.; Braschler, T.; Renaud, P.; Oliva, A.G. Label-free detection of *Babesia bovis* infected red blood cells using impedance spectroscopy on a microfabricated flow cytometer. *Acta Trop.* **2007**, *102*, 63–68. [[CrossRef](#)] [[PubMed](#)]
63. Holmes, D.; Pettigrew, D.; Reccius, C.H.; Gwyer, J.D.; van Berkel, C.; Holloway, J.; Davies, D.E.; Morgan, H. Leukocyte analysis and differentiation using high speed microfluidic single cell impedance cytometry. *Lab Chip* **2009**, *9*, 2881–2889. [[CrossRef](#)] [[PubMed](#)]
64. Han, X.J.; van Berkel, C.; Gwyer, J.; Capretto, L.; Morgan, H. Microfluidic Lysis of Human Blood for Leukocyte Analysis Using Single Cell Impedance Cytometry. *Anal. Chem.* **2012**, *84*, 1070–1075. [[CrossRef](#)]
65. Lei, K.F.; Chen, K.H.; Tsui, P.H.; Tsang, N.M. Real-Time Electrical Impedimetric Monitoring of Blood Coagulation Process under Temperature and Hematocrit Variations Conducted in a Microfluidic Chip. *PLoS ONE* **2013**, *8*, e76243. [[CrossRef](#)]
66. Song, H.J.; Wang, Y.; Rosano, J.M.; Prabhakarandian, B.; Garson, C.; Pant, K.; Lai, E. A microfluidic impedance flow cytometer for identification of differentiation state of stem cells. *Lab Chip* **2013**, *13*, 2300–2310. [[CrossRef](#)]
67. Du, E.; Ha, S.; Diez-Silva, M.; Dao, M.; Suresh, S.; Chandrakasan, A.P. Electric impedance microflow cytometry for characterization of cell disease states. *Lab Chip* **2013**, *13*, 3903–3909. [[CrossRef](#)] [[PubMed](#)]
68. Spencer, D.; Hollis, V.; Morgan, H. Microfluidic impedance cytometry of tumour cells in blood. *Biomicrofluidics* **2014**, *8*, 11. [[CrossRef](#)]
69. Liu, J.; Qiang, Y.H.; Alvarez, O.; Du, E. Electrical impedance microflow cytometry with oxygen control for detection of sickle cells. *Sens. Actuator B Chem.* **2018**, *255*, 2392–2398. [[CrossRef](#)]
70. Nguyen, T.A.; Yin, T.I.; Reyes, D.; Urban, G.A. Microfluidic Chip with Integrated Electrical Cell-Impedance Sensing for Monitoring Single Cancer Cell Migration in Three-Dimensional Matrixes. *Anal. Chem.* **2013**, *85*, 11068–11076. [[CrossRef](#)]
71. Liu, L.; Xiao, X.; Lei, K.F.; Huang, C.H. Quantitative impedimetric monitoring of cell migration under the stimulation of cytokine or anti-cancer drug in a microfluidic chip. *Biomicrofluidics* **2015**, *9*, 10. [[CrossRef](#)]
72. Huang, C.H.; Lei, K.F. Impedimetric quantification of migration speed of cancer cells migrating along a Matrigel-filled microchannel. *Anal. Chim. Acta* **2020**, *1121*, 67–73. [[CrossRef](#)] [[PubMed](#)]
73. Huang, C.H.; Lei, K.F. Quantitative study of tumor angiogenesis in three-dimensional matrigel barrier using electric impedance measurement technique. *Sens. Actuator B Chem.* **2022**, *370*, 8. [[CrossRef](#)]
74. Hong, J.L.; Lan, K.C.; Jang, L.S. Electrical characteristics analysis of various cancer cells using a microfluidic device based on single-cell impedance measurement. *Sens. Actuator B Chem.* **2012**, *173*, 927–934. [[CrossRef](#)]
75. Zhao, Y.; Zhao, X.T.; Chen, D.Y.; Luo, Y.N.; Jiang, M.; Wei, C.; Long, R.; Yue, W.T.; Wang, J.B.; Chen, J. Tumor cell characterization and classification based on cellular specific membrane capacitance and cytoplasm conductivity. *Biosens. Bioelectron.* **2014**, *57*, 245–253. [[CrossRef](#)] [[PubMed](#)]
76. Fan, W.H.; Chen, X.; Ge, Y.Q.; Jin, Y.; Jin, Q.H.; Zhao, J.L. Single-cell impedance analysis of osteogenic differentiation by droplet-based microfluidics. *Biosens. Bioelectron.* **2019**, *145*, 8. [[CrossRef](#)]
77. Lei, K.F.; Ho, Y.C.; Huang, C.H.; Huang, C.H.; Pai, P.C. Characterization of stem cell-like property in cancer cells based on single-cell impedance measurement in a microfluidic platform. *Talanta* **2021**, *229*, 8. [[CrossRef](#)] [[PubMed](#)]
78. Bieberich, E.; Guiseppi-Elie, A. Neuronal differentiation and synapse formation of PC12 and embryonic stem cells on interdigitated microelectrode arrays: Contact structures for neuron-to-electrode signal transmission (NEST). *Biosens. Bioelectron.* **2004**, *19*, 923–931. [[CrossRef](#)]
79. Jang, L.S.; Wang, M.H. Microfluidic device for cell capture and impedance measurement. *Biomed. Microdevices* **2007**, *9*, 737–743. [[CrossRef](#)]
80. Cho, Y.; Kim, H.S.; Frazier, A.B.; Chen, Z.G.; Shin, D.M.; Han, A. Whole-Cell Impedance Analysis for Highly and Poorly Metastatic Cancer Cells. *J. Microelectromech. Syst.* **2009**, *18*, 808–817. [[CrossRef](#)]
81. Hildebrandt, C.; Buth, H.; Cho, S.B.; Impidjati; Thielecke, H. Detection of the osteogenic differentiation of mesenchymal stem cells in 2D and 3D cultures by electrochemical impedance spectroscopy. *J. Biotechnol.* **2010**, *148*, 83–90. [[CrossRef](#)]
82. Houssin, T.; Folleta, J.; Follet, A.; Dei-Cas, E.; Senez, V. Label-free analysis of water-polluting parasite by electrochemical impedance spectroscopy. *Biosens. Bioelectron.* **2010**, *25*, 1122–1129. [[CrossRef](#)] [[PubMed](#)]
83. Dalmay, C.; Cheray, M.; Pothier, A.; Lalloue, F.; Jauberteau, M.O.; Blondy, P. Ultra sensitive biosensor based on impedance spectroscopy at microwave frequencies for cell scale analysis. *Sens. Actuator A Phys.* **2010**, *162*, 189–197. [[CrossRef](#)]
84. Bagnaninchi, P.O.; Drummond, N. Real-time label-free monitoring of adipose-derived stem cell differentiation with electric cell-substrate impedance sensing. *Proc. Natl. Acad. Sci. USA* **2011**, *108*, 6462–6467. [[CrossRef](#)]
85. Lei, K.F.; Wu, Z.M.; Huang, C.H. Impedimetric quantification of the formation process and the chemosensitivity of cancer cell colonies suspended in 3D environment. *Biosens. Bioelectron.* **2015**, *74*, 878–885. [[CrossRef](#)] [[PubMed](#)]
86. Chen, N.C.; Chen, C.H.; Chen, M.K.; Jang, L.S.; Wang, M.H. Single-cell trapping and impedance measurement utilizing dielectrophoresis in a parallel-plate microfluidic device. *Sens. Actuator B Chem.* **2014**, *190*, 570–577. [[CrossRef](#)]
87. Lei, K.F.; Kao, C.H.; Tsang, N.M. High throughput and automatic colony formation assay based on impedance measurement technique. *Anal. Bioanal. Chem.* **2017**, *409*, 3271–3277. [[CrossRef](#)]

88. Nguyen, N.V.; Jen, C.P. Impedance detection integrated with dielectrophoresis enrichment platform for lung circulating tumor cells in a microfluidic channel. *Biosens. Bioelectron.* **2018**, *121*, 10–18. [[CrossRef](#)]
89. Lei, K.F.; Lin, B.Y.; Tsang, N.M. Real-time and label-free impedimetric analysis of the formation and drug testing of tumor spheroids formed via the liquid overlay technique. *RSC Adv.* **2017**, *7*, 13939–13946. [[CrossRef](#)]
90. Lei, K.F.; Wu, M.H.; Hsu, C.W.; Chen, Y.D. Real-time and non-invasive impedimetric monitoring of cell proliferation and chemosensitivity in a perfusion 3D cell culture microfluidic chip. *Biosens. Bioelectron.* **2014**, *51*, 16–21. [[CrossRef](#)]
91. Sun, T.; Green, N.G.; Gawad, S.; Morgan, H. Analytical electric field and sensitivity analysis for two microfluidic impedance cytometer designs. *IET Nanobiotechnol.* **2007**, *1*, 69–79. [[CrossRef](#)] [[PubMed](#)]
92. Holmes, D.; She, J.K.; Roach, P.L.; Morgan, H. Bead-based immunoassays using a micro-chip flow cytometer. *Lab Chip* **2007**, *7*, 1048–1056. [[CrossRef](#)] [[PubMed](#)]
93. Sun, T.; Holmes, D.; Gawad, S.; Green, N.G.; Morgan, H. High speed multi-frequency impedance analysis of single particles in a microfluidic cytometer using maximum length sequences. *Lab Chip* **2007**, *7*, 1034–1040. [[CrossRef](#)]
94. Kummrow, A.; Theisen, J.; Frankowski, M.; Tuchscheerer, A.; Yildirim, H.; Brattke, K.; Schmidt, M.; Neukammer, J. Microfluidic structures for flow cytometric analysis of hydrodynamically focussed blood cells fabricated by ultraprecision micromachining. *Lab Chip* **2009**, *9*, 972–981. [[CrossRef](#)] [[PubMed](#)]
95. Spencer, D.; Morgan, H. Positional dependence of particles in microfluidic impedance cytometry. *Lab Chip* **2011**, *11*, 1234–1239. [[CrossRef](#)]
96. Barat, D.; Spencer, D.; Benazzi, G.; Mowlem, M.C.; Morgan, H. Simultaneous high speed optical and impedance analysis of single particles with a microfluidic cytometer. *Lab Chip* **2012**, *12*, 118–126. [[CrossRef](#)]
97. Spencer, D.; Elliott, G.; Morgan, H. A sheath-less combined optical and impedance micro-cytometer. *Lab Chip* **2014**, *14*, 3064–3073. [[CrossRef](#)] [[PubMed](#)]
98. Haandbaek, N.; Burgel, S.C.; Heer, F.; Hierlemann, A. Characterization of subcellular morphology of single yeast cells using high frequency microfluidic impedance cytometer. *Lab Chip* **2014**, *14*, 369–377. [[CrossRef](#)]
99. David, F.; Hebeisen, M.; Schade, G.; Franco-Lara, E.; Di Bernardino, M. Viability and membrane potential analysis of *Bacillus megaterium* cells by impedance flow cytometry. *Biotechnol. Bioeng.* **2012**, *109*, 483–492. [[CrossRef](#)]
100. Evander, M.; Ricco, A.J.; Morser, J.; Kovacs, G.T.A.; Leung, L.L.K.; Giovangrandi, L. Microfluidic impedance cytometer for platelet analysis. *Lab Chip* **2013**, *13*, 722–729. [[CrossRef](#)]
101. Lin, Z.; Cao, X.; Xie, P.; Liu, M.; Javanmard, M. PicoMolar level detection of protein biomarkers based on electronic sizing of bead aggregates: Theoretical and experimental considerations. *Biomed. Microdevices* **2015**, *17*, 7. [[CrossRef](#)] [[PubMed](#)]
102. Simon, P.; Frankowski, M.; Bock, N.; Neukammer, J. Label-free whole blood cell differentiation based on multiple frequency AC impedance and light scattering analysis in a micro flow cytometer. *Lab Chip* **2016**, *16*, 2326–2338. [[CrossRef](#)] [[PubMed](#)]
103. Xie, P.F.; Cao, X.N.; Lin, Z.T.; Javanmard, M. Top-down fabrication meets bottom-up synthesis for nanoelectronic barcoding of microparticles. *Lab Chip* **2017**, *17*, 1939–1947. [[CrossRef](#)] [[PubMed](#)]
104. McGrath, J.S.; Honrado, C.; Spencer, D.; Horton, B.; Bridle, H.L.; Morgan, H. Analysis of Parasitic Protozoa at the Single-cell Level using Microfluidic Impedance Cytometry. *Sci. Rep.* **2017**, *7*, 11. [[CrossRef](#)] [[PubMed](#)]
105. Tang, W.L.; Tang, D.Z.; Ni, Z.H.; Xiang, N.; Yi, H. Microfluidic Impedance Cytometer with Inertial Focusing and Liquid Electrodes for High-Throughput Cell Counting and Discrimination. *Anal. Chem.* **2017**, *89*, 3154–3161. [[CrossRef](#)]
106. Mansor, M.A.; Takeuchi, M.; Nakajima, M.; Hasegawa, Y.; Ahmad, M.R. Electrical Impedance Spectroscopy for Detection of Cells in Suspensions Using Microfluidic Device with Integrated Microneedles. *Appl. Sci.* **2017**, *7*, 170. [[CrossRef](#)]
107. Ahuja, K.; Rather, G.M.; Lin, Z.T.; Sui, J.Y.; Xie, P.F.; Le, T.; Bertino, J.R.; Javanmard, M. Toward point-of-care assessment of patient response: A portable tool for rapidly assessing cancer drug efficacy using multifrequency impedance cytometry and supervised machine learning. *Microsyst. Nanoeng.* **2019**, *5*, 11. [[CrossRef](#)]
108. Sui, J.Y.; Foflonker, F.; Bhattacharya, D.; Javanmard, M. Electrical impedance as an indicator of microalgal cell health. *Sci. Rep.* **2020**, *10*, 9. [[CrossRef](#)]
109. Mahesh, K.; Varma, M.; Sen, P. Double-peak signal features in microfluidic impedance flow cytometry enable sensitive measurement of cell membrane capacitance. *Lab Chip* **2020**, *20*, 4296–4309. [[CrossRef](#)]
110. Petchakup, C.; Hutchinson, P.E.; Tay, H.M.; Leong, S.Y.; Li, K.H.H.; Hou, H.W. Label-free quantitative lymphocyte activation profiling using microfluidic impedance cytometry. *Sens. Actuator B Chem.* **2021**, *339*, 9. [[CrossRef](#)]
111. Caselli, F.; Reale, R.; De Ninno, A.; Spencer, D.; Morgan, H.; Bisegna, P. Deciphering impedance cytometry signals with neural networks. *Lab Chip* **2022**, *22*, 1714–1722. [[CrossRef](#)] [[PubMed](#)]
112. Wang, R.H.; Wang, Y.; Lassiter, K.; Li, Y.B.; Hargis, B.; Tung, S.; Berghman, L.; Bottje, W. Interdigitated array microelectrode based impedance immunosensor for detection of avian influenza virus H5N1. *Talanta* **2009**, *79*, 159–164. [[CrossRef](#)] [[PubMed](#)]
113. Wang, R.H.; Lin, J.H.; Lassiter, K.; Srinivasan, B.; Lin, L.; Lu, H.G.; Tung, S.; Hargis, B.; Bottje, W.; Berghman, L.; et al. Evaluation study of a portable impedance biosensor for detection of avian influenza virus. *J. Virol. Methods* **2011**, *178*, 52–58. [[CrossRef](#)] [[PubMed](#)]
114. Shafiee, H.; Jahangir, M.; Inci, F.; Wang, S.Q.; Willenbrecht, R.B.M.; Giguel, F.F.; Tsibris, A.M.N.; Kuritzkes, D.R.; Demirci, U. Acute On-Chip HIV Detection Through Label-Free Electrical Sensing of Viral Nano-Lysate. *Small* **2013**, *9*, 2553–2563. [[CrossRef](#)]
115. Singh, R.; Hong, S.; Jang, J. Label-free Detection of Influenza Viruses using a Reduced Graphene Oxide-based Electrochemical Immunosensor Integrated with a Microfluidic Platform. *Sci. Rep.* **2017**, *7*, 11. [[CrossRef](#)]

116. Berdat, D.; Rodriguez, A.C.M.; Herrera, F.; Gijs, M.A.M. Label-free detection of DNA with interdigitated micro-electrodes in a fluidic cell. *Lab Chip* **2008**, *8*, 302–308. [[CrossRef](#)]
117. Javanmard, M.; Davis, R.W. A microfluidic platform for electrical detection of DNA hybridization. *Sens. Actuator B Chem.* **2011**, *154*, 22–27. [[CrossRef](#)]
118. Ben-Yoav, H.; Dykstra, P.H.; Bentley, W.E.; Ghodssi, R. A microfluidic-based electrochemical biochip for label-free diffusion-restricted DNA hybridization analysis. *Biosens. Bioelectron.* **2012**, *38*, 114–120. [[CrossRef](#)]
119. Chuang, C.H.; Du, Y.C.; Wu, T.F.; Chen, C.H.; Lee, D.H.; Chen, S.M.; Huang, T.C.; Wu, H.P.; Shaikh, M.O. Immunosensor for the ultrasensitive and quantitative detection of bladder cancer in point of care testing. *Biosens. Bioelectron.* **2016**, *84*, 126–132. [[CrossRef](#)]
120. Ondevilla, N.A.P.; Wong, T.W.; Lee, N.Y.; Chang, H.C. An AC electrokinetics-based electrochemical aptasensor for the rapid detection of microRNA-155. *Biosens. Bioelectron.* **2022**, *199*, 7. [[CrossRef](#)]
121. Wu, C.C.; Huang, W.C.; Hu, C.C. An ultrasensitive label-free electrochemical impedimetric DNA biosensing chip integrated with a DC-biased AC electroosmotic vortex. *Sens. Actuator B Chem.* **2015**, *209*, 61–68. [[CrossRef](#)]
122. Alsabbagh, K.; Hornung, T.; Voigt, A.; Sadir, S.; Rajabi, T.; Lange, K. Microfluidic Impedance Biosensor Chips Using Sensing Layers Based on DNA-Based Self-Assembled Monolayers for Label-Free Detection of Proteins. *Biosensors* **2021**, *11*, 80. [[CrossRef](#)] [[PubMed](#)]
123. Sheen, H.J.; Panigrahi, B.; Kuo, T.R.; Hsu, W.C.; Chung, P.S.; Xie, Q.Z.; Lin, C.Y.; Chang, Y.S.; Lin, C.T.; Fan, Y.J. Electrochemical biosensor with electrokinetics-assisted molecular trapping for enhancing C-reactive protein detection. *Biosens. Bioelectron.* **2022**, *210*, 9. [[CrossRef](#)]
124. Chinnadayala, S.R.; Cho, S. Electrochemical Immunosensor for the Early Detection of Rheumatoid Arthritis Biomarker: Anti-Cyclic Citrullinated Peptide Antibody in Human Serum Based on Avidin-Biotin System. *Sensors* **2021**, *21*, 124. [[CrossRef](#)] [[PubMed](#)]
125. Selvam, S.P.; Chinnadayala, S.R.; Cho, S. Electrochemical nanobiosensor for early detection of rheumatoid arthritis biomarker: Anti-cyclic citrullinated peptide antibodies based on polyaniline (PANI)/MoS<sub>2</sub>-modified screen-printed electrode with PANI-Au nanomatrix-based signal amplification. *Sens. Actuator B Chem.* **2021**, *333*, 12. [[CrossRef](#)]
126. Lin, C.Y.; Nguyen, U.T.N.; Hsieh, H.Y.; Tahara, H.; Chang, Y.S.; Wang, B.Y.; Gu, B.C.; Dai, Y.H.; Wu, C.C.; Tsai, I.J.; et al. Peptide-based electrochemical sensor with nanogold enhancement for detecting rheumatoid arthritis. *Talanta* **2022**, *236*, 9. [[CrossRef](#)]
127. Chiriaco, M.S.; Primiceri, E.; D'Amone, E.; Ionescu, R.E.; Rinaldi, R.; Maruccio, G. EIS microfluidic chips for flow immunoassay and ultrasensitive cholera toxin detection. *Lab Chip* **2011**, *11*, 658–663. [[CrossRef](#)]
128. Liu, F.; Nordin, A.N.; Li, F.; Voiculescu, I. A lab-on-chip cell-based biosensor for label-free sensing of water toxicants. *Lab Chip* **2014**, *14*, 1270–1280. [[CrossRef](#)]
129. Pradhan, R.; Kalkal, A.; Jindal, S.; Packirisamy, G.; Manhas, S. Four electrode-based impedimetric biosensors for evaluating cytotoxicity of tamoxifen on cervical cancer cells. *RSC Adv.* **2021**, *11*, 798–806. [[CrossRef](#)]
130. Guo, Y.M.; Liu, X.F.; Sun, X.; Cao, Y.Y.; Wang, X.Y. A PDMS Microfluidic Impedance Immunosensor for Sensitive Detection Of Pesticide Residues in Vegetable Real Samples. *Int. J. Electrochem. Sci.* **2015**, *10*, 4155–4164.
131. Zeng, L.; Wang, W.Q.; Rogers, F.; Zhang, H.P.; Zhang, X.M.; Yang, D.X. A High Sensitivity Micro Impedance Sensor Based on Magnetic Focusing for Oil Condition Monitoring. *IEEE Sens. J.* **2020**, *20*, 3813–3821. [[CrossRef](#)]
132. Lei, K.F.; Huang, C.H.; Tsang, N.M. Impedimetric quantification of cells encapsulated in hydrogel cultured in a paper-based microchamber. *Talanta* **2016**, *147*, 628–633. [[CrossRef](#)] [[PubMed](#)]
133. Teengam, P.; Siangproh, W.; Tuantranont, A.; Vilaivan, T.; Chailapakul, O.; Henry, C.S. Electrochemical impedance-based DNA sensor using pyrrolidiny peptide nucleic acids for tuberculosis detection. *Anal. Chim. Acta* **2018**, *1044*, 102–109. [[CrossRef](#)]
134. Rengaraj, S.; Cruz-Izquierdo, A.; Scott, J.L.; Di Lorenzo, M. Impedimetric paper-based biosensor for the detection of bacterial contamination in water. *Sens. Actuator B Chem.* **2018**, *265*, 50–58. [[CrossRef](#)]
135. Moazeni, M.; Karimzadeh, F.; Kermanpur, A. Peptide modified paper based impedimetric immunoassay with nanocomposite electrodes as a point-of-care testing of Alpha-fetoprotein in human serum. *Biosens. Bioelectron.* **2018**, *117*, 748–757. [[CrossRef](#)] [[PubMed](#)]
136. Lei, K.F.; Liu, T.K.; Tsang, N.M. Towards a high throughput impedimetric screening of chemosensitivity of cancer cells suspended in hydrogel and cultured in a paper substrate. *Biosens. Bioelectron.* **2018**, *100*, 355–360. [[CrossRef](#)]
137. Congur, G.; Erdem, A. PAMAM dendrimer modified screen printed electrodes for impedimetric detection of miRNA-34a. *Microchem. J.* **2019**, *148*, 748–758. [[CrossRef](#)]
138. Vasantham, S.; Alhans, R.; Singhal, C.; Nagabooshanam, S.; Nissar, S.; Basu, T.; Ray, S.C.; Wadhwa, S.; Narang, J.; Mathur, A. Paper based point of care immunosensor for the impedimetric detection of cardiac troponin I biomarker. *Biomed. Microdevices* **2019**, *22*, 9. [[CrossRef](#)]
139. Li, X.; Qin, Z.; Fu, H.; Li, T.; Peng, R.; Li, Z.J.; Rini, J.M.; Liu, X.Y. Enhancing the performance of paper-based electrochemical impedance spectroscopy nanobiosensors: An experimental approach. *Biosens. Bioelectron.* **2021**, *177*, 8. [[CrossRef](#)]
140. Kare, S.P.O.; Das, D.; Chaudhury, K.; Das, S. Hand-drawn electrode based disposable paper chip for artificial sweat analysis using impedance spectroscopy. *Biomed. Microdevices* **2021**, *23*, 12. [[CrossRef](#)]

141. Eksin, E.; Torul, H.; Yarali, E.; Tamer, U.; Papakonstantinou, P.; Erdem, A. Paper-based electrode assemble for impedimetric detection of miRNA. *Talanta* **2021**, *225*, 6. [[CrossRef](#)] [[PubMed](#)]
142. Karuppiyah, S.; Mishra, N.C.; Tsai, W.C.; Liao, W.S.; Chou, C.F. Ultrasensitive and Low-Cost Paper-Based Graphene Oxide Nanobiosensor for Monitoring Water-Borne Bacterial Contamination. *ACS Sens.* **2021**, *6*, 3214–3223. [[CrossRef](#)] [[PubMed](#)]
143. Yarali, E.; Eksin, E.; Torul, H.; Ganguly, A.; Tamer, U.; Papakonstantinou, P.; Erdem, A. Impedimetric detection of miRNA biomarkers using paper-based electrodes modified with bulk crystals or nanosheets of molybdenum disulfide. *Talanta* **2022**, *241*, 10. [[CrossRef](#)] [[PubMed](#)]
144. Mishra, A.; Pilloton, R.; Jain, S.; Roy, S.; Khanuja, M.; Mathur, A.; Narang, J. Paper-Based Electrodes Conjugated with Tungsten Disulfide Nanostructure and Aptamer for Impedimetric Detection of *Listeria monocytogenes*. *Biosensors* **2022**, *12*, 88. [[CrossRef](#)] [[PubMed](#)]
145. Furniturewalla, A.; Chan, M.; Sui, J.; Ahuja, K.; Javanmard, M. Fully integrated wearable impedance cytometry platform on flexible circuit board with online smartphone readout. *Microsyst. Nanoeng.* **2018**, *4*, 10. [[CrossRef](#)] [[PubMed](#)]
146. De Guzman, K.; Al-Kharusi, G.; Levingstone, T.; Morrin, A. Robust epidermal tattoo electrode platform for skin physiology monitoring. *Anal. Methods* **2019**, *11*, 1460–1468. [[CrossRef](#)]
147. Lee, H.B.; Meeseepong, M.; Trung, T.Q.; Kim, B.Y.; Lee, N.E. A wearable lab-on-a-patch platform with stretchable nanostructured biosensor for non-invasive immunodetection of biomarker in sweat. *Biosens. Bioelectron.* **2020**, *156*, 8. [[CrossRef](#)]
148. Huynh, V.L.; Trung, T.Q.; Meeseepong, M.; Lee, H.B.; Nguyen, T.D.; Lee, N.E. Hollow Microfibers of Elastomeric Nanocomposites for Fully Stretchable and Highly Sensitive Microfluidic Immunobiosensor Patch. *Adv. Funct. Mater.* **2020**, *30*, 12. [[CrossRef](#)]
149. Nah, J.S.; Barman, S.C.; Abu Zahed, M.; Sharifuzzaman, M.; Yoon, H.; Park, C.; Yoon, S.; Zhang, S.P.; Park, J.Y. A wearable microfluidics-integrated impedimetric immunosensor based on Ti3C2Tx MXene incorporated laser-burned graphene for noninvasive sweat cortisol detection. *Sens. Actuator B Chem.* **2021**, *329*, 9. [[CrossRef](#)]

**Disclaimer/Publisher's Note:** The statements, opinions and data contained in all publications are solely those of the individual author(s) and contributor(s) and not of MDPI and/or the editor(s). MDPI and/or the editor(s) disclaim responsibility for any injury to people or property resulting from any ideas, methods, instructions or products referred to in the content.